1952

Investigation of transients in an analogue circuit for an ignitron motor control system

Bryant, Carleton Fanton; Adams, Clayton Rand.

Ohio State University

INVESTIGATION OF TRANSIENTS IN AN ANALOGUE CIRCUIT FOR AN IGNITRON MOTOR CONTROL SYSTEM

CARLETON FANTON BRYANT, JR.
CLAYTON RAND ADAMS

INVESTIGATION OF TRANSIENTS IN AN ANALOGUE CIRCUIT FOR AN IGNITRON MOTOR CONTROL SYSTEM

by

Carleton Fanton Bryant, Jr., Lieutenant Commander, U. S. Navy
B.S., Massachusetts Institute of Technology, 1943.
Clayton Rand Adams, Lieutenant (j.g.), U. S. Navy
B.S., U. S. Naval Academy, 1947.

Submitted in Partial Fulfillment
of the Requirements for the
Degree of Naval Engineer

From the
Massachusetts Institute of Technology
1952

ABSTRACT

INVESTIGATION OF TRANSIENTS IN AN ANALOGUE CIRCUIT FOR AN IGNITRON MOTOR CONTROL SYSTEM

by

Carleton F. Bryant, Jr.
Clayton R. Adams

Submitted to the Department of Naval Architecture and Marine Engineering on 15 May 1952 in partial fulfillment of the requirements for the degree of Naval Engineer.

This thesis is a continuation of an investigation of transient speed characteristics of an ignitron-fed d-c motor undertaken by P. N. Heller, which consisted of actual tests on a 15 horsepower motor with a 3-phase ignitron rectifier and the development of two analytical methods of predicting the transient behavior. Because of the involved calculations required for the analytical methods and the difficulties of conducting full scale tests, it was proposed that an analogue circuit be used for future tests of this type.

The primary purpose of this investigation was the construction, testing, and evaluation of this analogue circuit. It was found that the usefulness of the analogue was limited by a transient current occurring during discontinuous conduction at the termination of each current pulse causing the analogue to misrepresent actual ignitron and motor performance in the boundary region between continuous and discontinuous conduction.

It was also found during the course of the investigation, however, that the transient response of the system could be predicted with reasonable accuracy using an exponential time constant approach which involves considerably less computational work than the previous methods.

Thesis Supervisor: Alexander Kusko

Title: Assistant Professor of Electrical Engineering

ABSTRACT

Submitted to the Department of Naval Architecture and Marine Engineering on May 1952 in partial fulfillment of the requirements for the degree of Naval Engineer.

This thesis is a continuation of an investigation of transient speed characteristics of an ignition-fed d-c motor undertaken by I. N. Muller, which consisted of actual tests on a 15 horsepower motor with a 3-phase ignition rectifier and the development of two analytical methods of predicting the transient behavior. Because of the involved calculations required for the analytical methods and the difficulties of conducting full scale tests, it was proposed that an analogue circuit be used for future tests of this type.

The primary purpose of this investigation was the construction, testing, and evaluation of this analogue circuit. It was found that the usefulness of the analogue was limited by a transient current occurring during discontinuous conduction at the termination of each current pulse causing the analogue to misrepresent actual ignition and motor performance in the boundary region between continuous and discontinuous conduction.

It was also found during the course of the investigation, however, that the transient response of the system could be predicted with reasonable accuracy using an exponential time constant approach which involves considerably less computational work than the previous methods.

Thesis Supervisor: Alexander Kusko

Title: Assistant Professor of Electrical Engineering

Cambridge, Massachusetts

May 15, 1952

Secretary of the Faculty
Massachusetts Institute of Technology
Cambridge, Massachusetts

Dear Sir:

In accordance with the requirements for the Degree of Naval Engineer, we submit herewith a thesis entitled "Investigation of Transients In An Analogue Circuit For An Ignitron Motor Control System".

Respectfully,

Carleton F. Bryant, Jr.
Lieutenant Commander
U. S. Navy

Clayton R. Adams
Lieutenant, (j.g.)
U. S. Navy

Cambridge, Massachusetts

May 15, 1952

Secretary of the Faculty
Massachusetts Institute of Technology
Cambridge, Massachusetts

Dear Sir:

In accordance with the requirements for the Degree of Naval Engineer, we submit herewith a thesis entitled: "Investigation of Transients in an Analogue Circuit for an Ignitron Motor Control System".

Respectfully,

Clifton T. Bryant, Jr.
Lieutenant Commander
U. S. Navy

Olaf Von N. Adams
Lieutenant, (J.G.)
U. S. Navy

ACKNOWLEDGEMENTS

The authors wish to express their appreciation to Professor Alexander Kusko for his advice and encouragement; and to Mr. P. N. Heller for his helpful suggestions.

The authors wish to express their appreciation to
Professor Alexander Dunlop for his advice and encouragement;
and to Mr. F. B. Heller for his helpful suggestions.

TABLE OF CONTENTS

Table of Contents

INTRODUCTION

Direct-current motors connected to a-c power supplies through grid-controlled rectifiers are being used at the present time for power applications requiring a wide range of speed control. Single-phase full-wave thyratron rectifiers are generally used for fractional horsepower installations, while three-phase ignitron rectifiers are used for the higher ratings.

Speed control of the motor is obtained by changing the firing angle of the rectifier. The system is a substitute for a Ward-Leonard type of control with the rectifier replacing the d-c generator, although the governing action of the ignitrons or thyratrons is probably more analogous to throttling in a mechanical power device.

While the steady state operation of this type of electronic drive has been rather fully investigated,[1) 2) 3)] relatively little has been published dealing with the transient behavior of the system for major changes of speed or load.

---

1) Vedder, E. H. and Puchlowski, K. P., "Theory of Rectifier D-C Motor Drive", AIEE Trans., 62, 1943, pages 863-870.

2) Schmidt, A. and Smith, W. P., "Operation of Large D-C Motors from Controlled Rectifiers", AIEE Trans., 67, 1948, pages 679-683.

3) Chute, G. M., "Electronic Motor and Welder Controls", McGraw-Hill Book Co., 1951, pages 191-202, 226-277.

INTRODUCTION

Direct-current motors connected to a-c power supplies through grid-controlled rectifiers are being used at the present time for power applications requiring a wide range of speed control. Single-phase full-wave thyratron rectifiers are generally used for fractional horsepower installations, while three-phase ignitron rectifiers are used for the higher ratings.

Speed control of the motor is obtained by changing the firing angle of the rectifier. The system is a substitute for a Ward-Leonard type of control with the rectifier replacing the d-c generator, although the governing action of the ignitrons or thyratrons is probably more analogous to throttling in a mechanical power device.

While the steady state operation of this type of electronic drive has been rather fully investigated, 1) 2) 3) relatively little has been published dealing with the transient behavior of the system for major changes of speed or load.

1) Vedder, E. H. and Puchlowski, K. P., "Theory of Rectifier D-C Motor Drive", AIEE Trans., 62, 1943, pages 863-870.

2) Schmidt, A. and Smith, R. C., "Operation of Large D-C Motors from Controlled Rectifiers", AIEE Trans., 67, 1948, pages 675-683.

3) Chute, G. M., "Electronic Motor and Welder Controls", McGraw-Hill Book Co., 1951, pages 191-202, 226-277.

This thesis is a continuation of an investigation of transient speed characteristics of an ignitron-fed d-c motor undertaken by P. N. Heller,[4] which consisted of actual tests on a 15 horsepower motor with a 3-phase ignitron rectifier and the development of two analytical methods of predicting the transient behavior. Because of the involved calculations required for the analytical methods and the difficulties of conducting full scale tests, it was proposed that an analogue circuit be used for future tests of this type.

The primary purpose of this investigation was the construction, testing, and evaluation of this analogue circuit. It was also found during the course of the investigation, however, that the transient response of the system could be predicted with reasonable accuracy using an exponential time constant approach which involves considerably less computational work than the previous methods. In the presentation which follows, these two aspects will be considered separately.

---

4) Heller, P. N., "Transient Speed and Armature Current Characteristics of an Ignitron-Fed D-C Motor". M.I.T. E.E. Dept. Thesis 1951.

This thesis is a continuation of an investigation of transient speed characteristics of an induction-type d-c motor undertaken by R. Keller,[1] which considered of course two a 1½ horsepower motor with a 3-phase induction rectifier and the derivation of two analytical methods of predicting the transient behavior. Because of the involved calculations required for the analytical methods and the difficulties of procuring full scale tests, it was proposed that an electronic circuit be used for future tests of this type.

The primary purpose of this investigation was the construction, testing, and evaluation of this analogue circuit. It was also found during the course of the investigation, that the transient response of the system could be predicted with reasonable accuracy using an exponential time constant obtained within laboratory time computational work time the previous methods. In the succeeding section which follows, these two aspects will be considered separately.

---

[1] Keller, R. E., "Transient Speed and Armature Current Characteristics of an Induction-Fed D-C Motor". M.I.T. E.E. Dept. Thesis 1951.

DERIVATION OF THE ANALOGUE CIRCUIT

The analogue circuit used for this investigation was intended to represent the 15 horsepower separately excited d-c shunt motor and the 3-phase ignitron rectifier used by Heller in obtaining experimental speed response curves for step changes in firing angle.[4] The name-plate data of these units together with the generator used for loading the system is given in Appendix A.

Mechanical-Electrical Equivalents.

The actual circuit studied is shown in Figure 1. The justification for the electrical representation of the mechanical motor characteristics may be shown by the following analysis in which the air gap flux is considered constant (constant shunt field current with armature reaction neglected).

The electrical relationship is

$$v_t = L_a \frac{di_a}{dt} + i_a R_a + V_b + e_b \qquad (1)$$

where v_t = voltage applied to armature circuit.

i_a = armature current

e_b = counter-emf (voltage between points d and e of Figure 1.)

V_b = brush drop (absorbed with tube drop in circuit)

R_a = armature resistance

L_a = armature inductance

t = time

The instantaneous air-gap torque of the motor rigidly coupled to a load with linear characteristics is given by

DESCRIPTION OF THE ANALOGUE CIRCUIT

The analogue circuit used for this investigation was intended to represent the 15 horsepower repulsion motor used by A-C mines motor and the 3-phase induction generator used by Heller in obtaining extrapolated blown recharge curves for step changes in firing angle. [4] The same-plate duds of those units together with the generator used for locating the system is given in Appendix A.

Mathematical Equivalence.

The actual circuit studied is shown in Figure 1. The justification for the electrical representation of the mechanical motor characteristics may be shown by the following analysis in which the air gap flux is considered constant (constant mmf field current with armature reaction neglected).

The electrical reliability is

$$e^a = Ie \frac{d\psi^a}{dt} + \dot{z}^a \psi^a + \lambda^b + e^b \qquad (1)$$

where λ^a = voltage equation in armature circuit.

i^a = armature current

e^a = counter-emf (voltage between points a and a of figure 1.)

λ^b = brush drop (opposed when this drop is steady)

t = time

i^e = effective inductance

ψ^a = armature reluctance

$\dot{z}^a$ = armature current

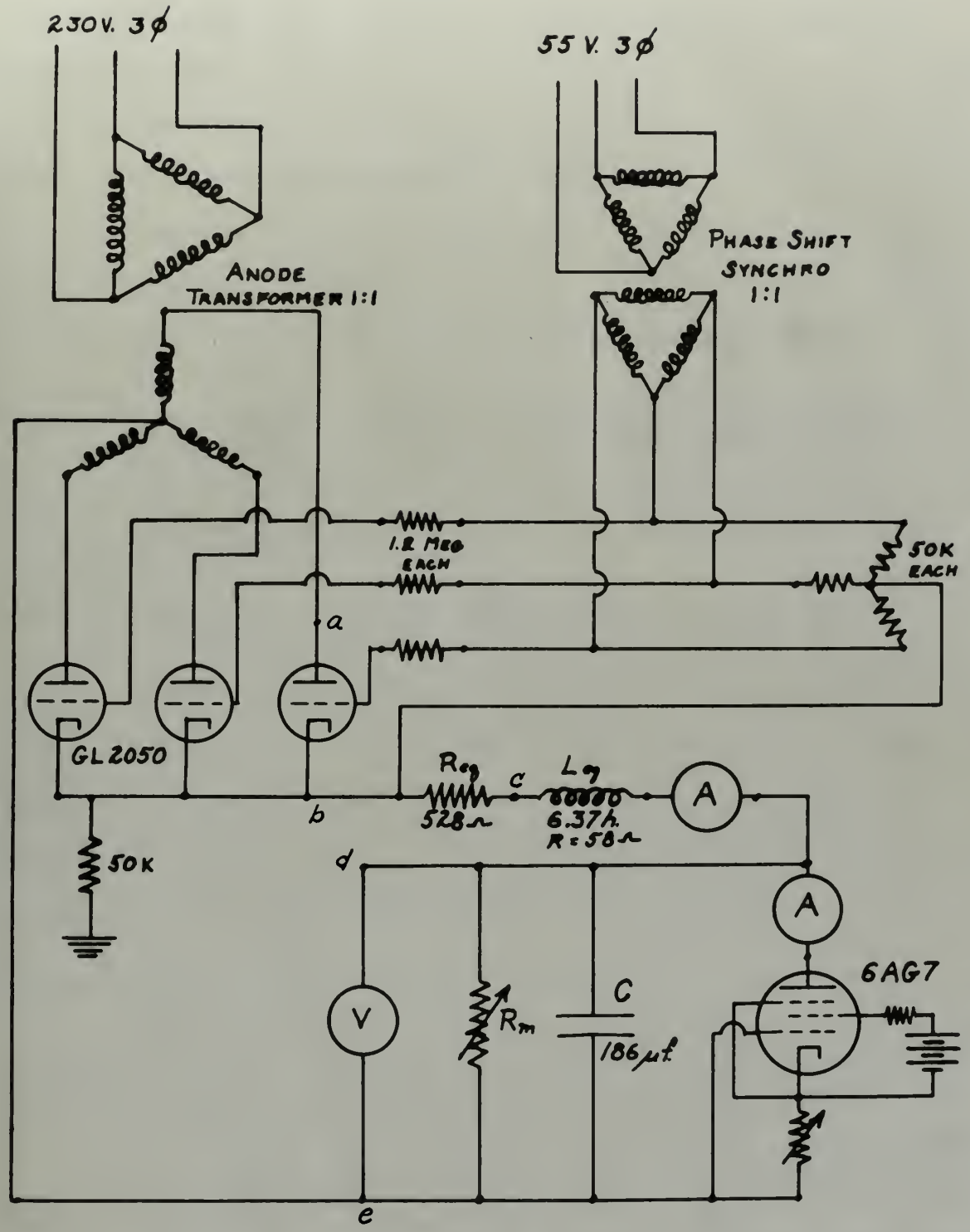

ANALOGUE CIRCUIT DIAGRAM

FIG 1

C70
5/2/52

$$(J_L + J_a)\frac{dw}{dt} + (B_L + B_a)\, w + T_L + T_a = T_{ag} \qquad (2)$$

Here

w = Motor speed

T_{ag} = instantaneous air-gap torque

J_L = load inertia

J_a = armature inertia

B_L = component of load torque which is proportional to speed.

B_a = coefficient of those components of motor friction, windage, and core-loss torque which are proportional to speed.

T_L = component of load torque which is constant at all speeds.

T_a = hysteresis and other rotational loss torques of the motor which are constant at all speeds.

The counter-emf of the motor is directly proportional to the product of motor speed and air-gap flux; the air-gap torque is directly proportional to the product of armature current and air-gap flux. It is assumed that the air-gap flux of the shunt motor is constant and that hence

$$e_b = k_1 w \qquad (3)$$

$$T_{ag} = k_2 i_a \qquad (4)$$

The electro-mechanical coupling constants k_1 and k_2 can be determined from test or design data of the motor.

Equation (2) can be translated into electrical terms by substituting $\frac{e_b}{k_1}$ for w and $k_2 i_a$ for T_{ag}, giving,

$$\frac{J_L + J_a}{k_1 k_2}\,\frac{de_b}{dt} + \frac{B_L + B_a}{k_1 k_2}\, e_b + \frac{T_L + T_a}{k_2} = i_a \qquad (5)$$

$$(q^f + \zeta^a)\frac{\gamma\phi}{\gamma t} + (b^f + b^a)\omega + \lambda^f + T^a = T^{ag} \qquad (2)$$

Here

ω = motor speed

T^{ag} = instantaneous air-gap torque

λ^f = load inertia

ζ^a = armature inertia

b^f = component of load torque which is proportional to speed.

b^a = coefficient of those components of motor friction, windage, and core-loss torque which are proportional to speed.

λ^f = component of load torque which is constant at all speeds.

T^a = hysteresis and other rotational loss torques of the motor which are constant at all speeds.

The counter-emf of the motor is directly proportional to the product of motor speed and air-gap flux; the air-gap torque is directly proportional to the product of armature current and air-gap flux. It is assumed that the air-gap flux of the shunt motor is constant and that hence

$$T^{ag} = K_2 i^a \qquad (4)$$

$$e^b = K_1 \phi_m \qquad (3)$$

The electro-mechanical coupling constants c^f and b^f can be determined from test or design data of the motor.

Equation (2) can be transformed into standard terms by substituting $\frac{K_1}{e^b}$ for ω and $K_2 i^a$ for T^{ag}, giving,

$$\frac{K_1 K_2}{q^f + \zeta^a}\frac{\gamma\phi}{\gamma t} + \frac{K_1 K_2}{b^f + b^a}e^b + \frac{\lambda^2}{b^f + \lambda^a} = i^a \qquad (5)$$

This last equation describes the behavior of the parallel circuit between points d and e of Figure 1 if

$$C = \frac{J_L + J_a}{k_1 k_2} \qquad (6)$$

$$R_m = \frac{k_1 k_2}{B_L + B_a} \qquad (7)$$

$$i_{L1} = \frac{T_L + T_a}{k_2} \qquad (8)$$

The 6AG7 pentode with cathode bias represents the current cource i_{L1} while the GL 2050 thyratrons simulate the ignitron rectifier.

Scale Ratios.

The scale ratios between motor and analogue are most easily obtained by expressing voltages, currents and impedances as per unit values. Base values taken were the anode transformer secondary rms voltage and the armature current. No attempt was made to change the time scale since the only three phase power available was 60 cycle.

Choice of the Analogue Circuit Elements.

In order to keep the effects of tube voltage drop of the same order of magnitude in both the analogue circuit and the actual rectifier, 220 volts was used for the anode transformer secondary voltage. Type GL 2050 thyratrons were chosen for the rectifier since they have the necessary inverse voltage and average and peak current ratings for the circuit and were readily available. The current level of the circuit was

This last equation describes the behavior of the parallel circuit between points d and e of Figure 1 if

$$(6) \qquad C = \frac{r_1 + r_2}{R_1 R_2}$$

$$(7) \qquad R_d = \frac{r_1 r_2}{r_1 + r_2}$$

$$(8) \qquad I_L = \frac{E_1 + E_2}{R_2}$$

The 6AG7 pentode with cathode bias represents the current source I_L while the GL 2050 thyratrons simulate the ignitron rectifier.

Scale Ratios.

The scale ratios between motor and analogue are most easily obtained by expressing voltages, currents and impedances as per unit values. Base values taken were the anode transformer secondary rms voltage and the armature current. No attempt was made to change the time scale since the only three phase power available was 60 cycle.

Choice of the Analogue Circuit Elements.

In order to keep the effects of tube voltage drop of the same order of magnitude in both the analogue circuit and the actual rectifier, 230 volts was used for the anode transformer secondary voltage. Type GL 2050 thyratrons were chosen for the rectifier since they have the necessary inverse voltage and average and peak current ratings for the circuit and were readily available. The current level of the circuit was

determined by the capacity of available vacuum tubes used for the current source. By using two 6AG7 pentodes in parallel it was possible to pass about 60 milliamperes, giving a ratio of actual motor current to analogue current of about 1000 to 1.

The impedance level of the analogue was actually determined by the iron-core reactor used to represent the armature inductance and the anode transformer leakage inductance. Available units were tested by obtaining magnetization curves with 60 cycle current up to a value of about 70 ma. The unit chosen indicated no saturation up to this point. A laboratory capacitor unit was adjusted and tested in the same manner to give the desired value of capacitance for the circuit. The motor and analogue circuit element values are listed in Table I.

Transformers.

The anode transformer used was a bank of three 5 KVA 110/220 to 110/220 single phase power transformers. Since the leakage inductance and resistance of these units is negligible on the basis of the analogue circuit the equivalent leakage inductance and resistance of the actual rectifier transformer has been lumped with the armature resistance and inductance of the motor. This is not strictly accurate since the transformer equivalents should appear in the input circuit to the thyratrons, but the results are not considered to be affected appreciably by this approximation.

The phase shift circuit was supplied by reduced voltages taken from a bank of transformers similar to the anode trans-

TABLE I

MOTOR AND ANALOGUE CIRCUIT ELEMENT VALUES

Element	Motor	Per Unit	Analogue
Anode Transformer Secondary Voltage	232 v.	1.00	220 v.
Motor-Rated Current	56 a.	1.00	0.0518 a.
Armature Resistance (60 cycle a-c)	0.484 Ω	0.117	495 Ω
Transformer Resistance	0.089 Ω	0.0215	91 Ω
Armature Inductance	5.84×10^{-3} h.	1.41×10^{-3}	5.97 h.
Transformer Leakage Inductance	0.39×10^{-3} h.	0.094×10^{-3}	0.40 h.
Equivalent Motor Inertia	0.190± 5% f.	0.79	186×10^{-6} f.

Motor data taken from reference 4.

Table I

Values for Various Circuit Elements Used

Element	Value	Per Unit	Location
Single Transformer Secondary Voltage	237 V.	1.00	237 V.
Rotor-Wound Current	31 A.	1.00	0.0318 A.
Armature Resistance (60 cycle e-c)	0.186 Ω	0.117	588 Ω
Transformer Resistance	0.089 Ω	0.0415	28 Ω
Armature Inductance	5.04×10^{-3} H.	1.41×10^{-3}	3.97 H.
Transformer Inductance	0.9×10^{-3} H.	0.254×10^{-3}	0.60 H.
Equivalent motor Inertia	0.1344 sec-ft.	0.79	186×10^{-6} F.

Motor data used from reference 4.

former. The phase shift transformer was a small synchro rated at 96/96 volts. This was provided with a dial and calibrated to read phase shift directly by comparing the output with the thyratron supply voltage on an oscilloscope. Observation indicated that the phase shift as read from the synchro dial was accurate within about two degrees.

from the synchro dial was accurate within about two thirds.
scope. Observation indicated that the phase shift at rest
output with sine function supply voltage on an oscillo-
calibrated by read phase shift directly by comparing the
rated at 90/90 volts. This was provided with a dial and
trimmer. The phase shift transformer was a small straight

OPERATION OF THE ANALOGUE CIRCUIT

Current Cutoff Transient.

The principle difficulty experienced with the analogue circuit occurred during discontinuous conduction. When each pulse of current cut off an underdamped current oscillation occurred which had a peak value of up to 10% of the current pulse itself and extended for about one-sixth cycle of the applied voltage. This resulted in unstable operation of the circuit in the region between continuous and discontinuous conduction. No means was found of appreciably reducing the magnitude of the oscillation, but by introducing a 50,000 ohm resistor in the ground circuit, it was damped out much more rapidly. It was not found possible however, to eliminate the resulting instability of the circuit.

Steady-State Characteristics.

Tests were made with the circuit to determine both the steady-state and transient performance. Steady-state curves of counter-emf versus armature current were obtained for various firing angles by reading the direct current in the circuit with a d'Arsonval type milliammeter and the voltage between points d and e on Figure 1 with a d-c voltmeter. The values obtained are shown on Figure 2 reduced to a per unit basis and corrected for variations in supply voltage.

Transient Characteristics.

The transient behavior of the counter-emf (speed) for step changes in firing angle was investigated by obtaining

Current Pulse Technique.

The primary difficulty experienced with the analogue circuit concerned erratic discontinuous conduction. Each odd pulse of current put off an unwanted output oscillation obtained which had a peak value of up to 10% of the current pulse itself and extended for about one-sixth cycle of the applied voltage. This resulted in unreliable operation of the circuit in the region between continuous and discontinuous conduction. In order to find or appreciably reduce the variations of the conditions, due to introducing a 30,000 ohm resistor in the ground circuit, it was decided out most safe really. It was not found possible however, to eliminate the resulting instability of the circuit.

Steady-State Characteristics.

Tests were made with the circuit to determine both the steady-state and transient performance. Thereby-mixed curves of sawtooth-out voltage pressure current were obtained for various pulse widths by varying the firing current in the circuit with a 3-terminal type milliammeter and the voltage between points B and E on Figure I with a d-a voltmeter. The values obtained are shown on Figure 2 reduced to a per unit basis and portrayed for variations in supply voltage.

Transient Characteristics.

The transient behavior of the sawtooth-out (pulse) for step changes in firing angle was investigated by operating

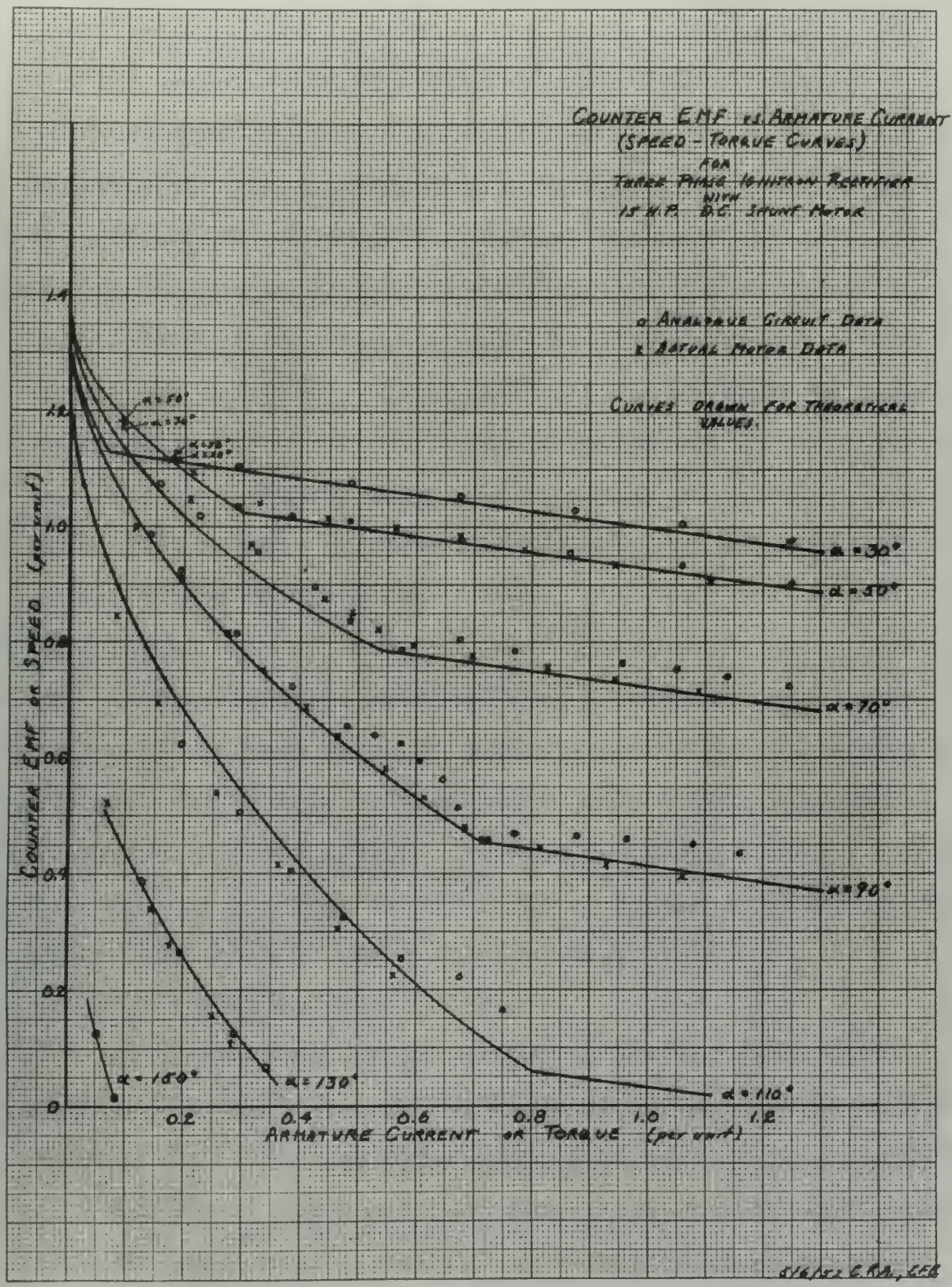
COUNTER EMF vs ARMATURE CURRENT
(SPEED - TORQUE CURVES)
FOR
THREE PHASE IGNITRON RECTIFIER
WITH
15 H.P. D.C. SHUNT MOTOR
o ANALYZER CIRCUIT DATA
x ACTUAL MOTOR DATA
CURVES DRAWN FOR THEORETICAL VALUES.
COUNTER EMF or SPEED (per unit)
ARMATURE CURRENT or TORQUE (per unit)
α = 30°
α = 50°
α = 70°
α = 90°
α = 110°
α = 130°
α = 150°
1.4
1.2
1.0
0.8
0.6
0.4
0.2
0
0.2
0.4
0.6
0.8
1.0
1.2

FIG 2

overall response times to reach 95% of the final value for conditions simulating those under which corresponding data for the actual motor was previously obtained by Heller.[4] The step changes in firing angle were introduced by manually rotating the phase shift synchro between stops to give the desired angles. The speed transient was observed on an oscilloscope connected between points d and e on Figure 1, with a calibrated sweep frequency to give about ten traces during the transient. The response time was obtained merely by counting the number of traces required for the counter-emf to reach the required value and hence may be somewhat inaccurate. The results of these measurements are compared with Heller's data in Table II.

Wave Forms.

Photographs were obtained with a polaroid oscilloscope camera of the wave forms of current, motor terminal voltage, and plate to cathode voltage under various operating conditions with the oscilloscope connected between points b and c, b and e, and a and b, respectively on Figure 1. These photographs are shown on Figures 3, 4, and 5.

Comparative Motor Tests.

In order to determine whether or not the instability found in the operation of the analogue circuit in the region between continuous and discontinuous conduction also occurred with the actual motor and rectifier, tests were made to determine the steady-state counter-emf versus armature current curves for the actual unit. The counter-emf, E_b, was deter-

overall response time is taken 95% of the final value for conditions exemplified there under which extraordinary data for the second sweep are obviously obtained by Keller.[4]

The step changes in Trig. angle were introduced by manually rotating the phase shift transformer shown to give the desired angles. The speed throughout was obtained on an oscilloscope connected between points $\underline{g}$ and $\underline{c}$ of Figure 1, with a calibrated sweep frequency to give four traces during one revolution. The response time was obtained naturally by counting the number of traces required for the counter-emf to reach the required value and hence may be subsequent interpolate. The results of these measurements are compared with Keller's data in Table II.

Wave Forms.

Photographs were obtained with a potential oscilloscope across of the wave form of current, motor terminal voltage, and plate to cathode voltage under various operating conditions with the oscilloscope connected between points $\underline{b}$ and $\underline{o}$, $\underline{b}$ and $\underline{a}$, and $\underline{b}$ and $\underline{d}$, respectively on Figure 1. These photographs are shown on Figure 3, 4, and 5.

Comparative Motor Tests.

In order to determine whether or not the instability found in the operation of the conclave circuit in the region between excitrons and discontinuous conduction time measurements with the motor and rectifier, tests were made to determine the steady-state current-volt internal characteristics for the motor unit. The counter-emf, E_b, was deter-

TABLE II

TRANSIENT RESPONSE TIME COMPARISON DATA

Run	Speed (rpm)		Angle (degrees)		Motor Response Time (Sec.)	Analogue Response Time (Sec.)
	Initial	Final	Initial	Final		
J-1	902	320	96	135	11.2	11
J-2	460	742	127	109	4.0	4.7
K-1	205	430	137	121	3.2	3.8
K-2	728	465	97	120	4.0	4.2
L-1	490	210	106	132	2.3	3.0
L-2	365	590	118	97	1.4	1.9
L-3	625	810	96	72	1.0	0.2
L-4	842	580	66	102	2.0	1.7
M-1	460	672	105	81	1.1	1.2
M-2	710	501	78	102	1.7	1.7
M-3	460	565	---	97	1.2	1.3
M-4	0	255	180	126	1.7	2.0
N-1	408	825	105	62	0.32	0.32
N-2	830	388	60	109	1.6	1.6
P-1	715	885	70	52	0.34	0.3
P-2	770	410	67	101	1.5	1.2
P-3	880	680	52	74	0.57	0.7
Q-1	535	750	85	65	0.26	0.25
Q-2	875	778	51	63	0.30	0.20

Motor data taken from reference 4.

Table II

Run	Speed (rpm)		Accts (accepted)		Accept Time (sec)	Loading Time (sec)
	Initial	Final	Failed	Time		
I-1	902	382	99	339	12.3	12
I-2	460	742	147	109	4.0	4.7
K-1	209	430	147	121	3.2	3.8
K-2	732	465	92	130	4.0	4.2
L-1	490	210	106	132	3.3	3.8
L-2	385	590	118	97	1.4	1.9
L-3	656	810	84	72	1.0	0.2
L-4	842	580	66	102	2.0	1.7
M-1	460	672	105	81	1.1	1.2
M-2	710	501	78	102	1.7	4.7
M-3	160	505	---	97	1.3	1.3
C-4	0	855	140	124	1.7	5.0
C-1	408	895	105	62	0.20	0.34
B-2	870	300	60	102	1.6	1.0
F-1	715	885	70	32	0.34	0.3
B-2	710	470	67	101	1.3	1.2
I-3	880	600	52	74	0.37	0.7
Q-1	535	740	52	65	0.20	0.25
E-2	675	726	81	103	0.34	0.20

Budget data taken from reference 4.

FIG 3 — ARMATURE VOLTAGE WAVEFORM

ANALOGUE

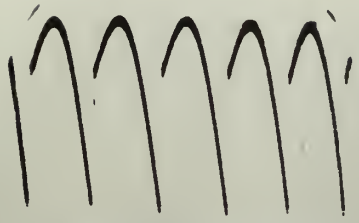

$\alpha = 50°$ $I_a = 52$ ma

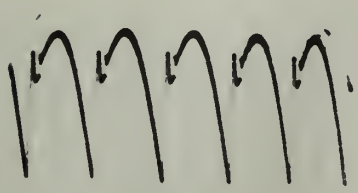

$\alpha = 50°$ $I_a = 11$ ma.

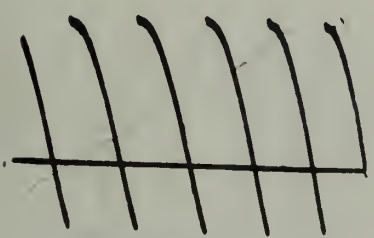

$\alpha = 90°$ $I_a = 52$ ma.

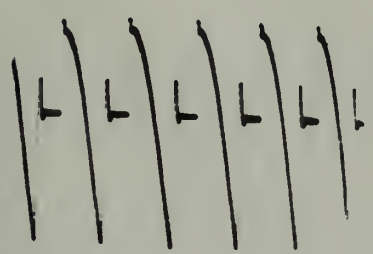

$\alpha = 90°$ $I_a = 9$ ma.

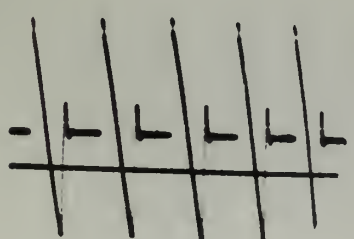

$\alpha = 140°$ $I_a = 5.7$ ma.

MOTOR

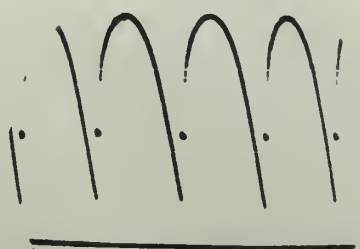

$\alpha = 50°$ $I_a = 56$ a

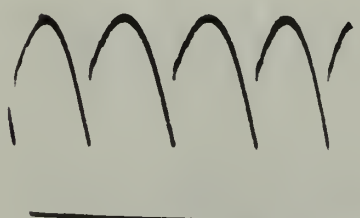

$\alpha = 50°$ $I_a = 12$ a.

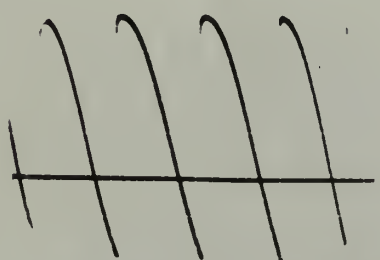

$\alpha = 90°$ $I_a = 56$ a.

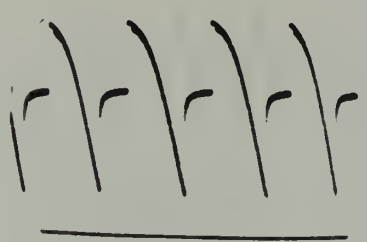

$\alpha = 90°$ $I_a = 10$ a

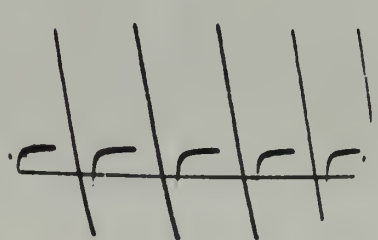

$\alpha = 140°$ $I_a = 6$ a.

FIG 4 — ARMATURE CURRENT WAVEFORM

ANALOGUE

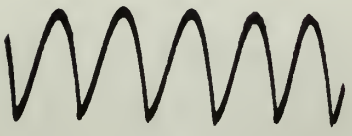

$\alpha = 50°$ $I_a = 52$ ma.

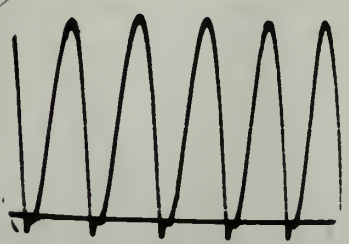

$\alpha = 50°$ $I_a = 11$ ma

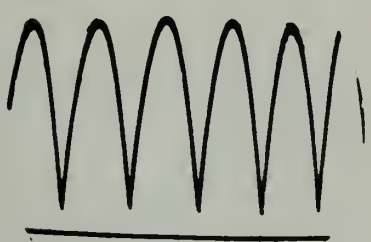

$\alpha = 90°$ $I_a = 52$ ma

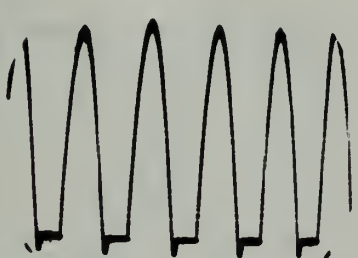

$\alpha = 90°$ $I_a = 9$ ma.

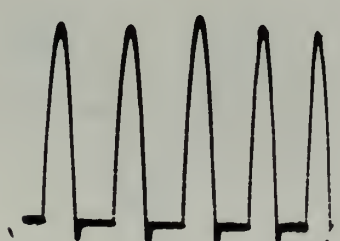

$\alpha = 140°$ $I_a = 5.7$ ma.

MOTOR

$\alpha = 50°$ $I_a = 56$ a.

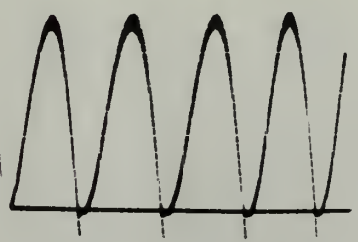

$\alpha = 50°$ $I_a = 12$ a.

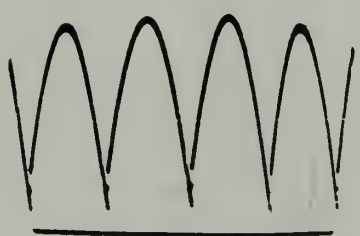

$\alpha = 90°$ $I_a = 56$ a.

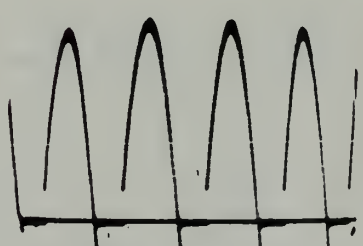

$\alpha = 90°$ $I_a = 10$ a.

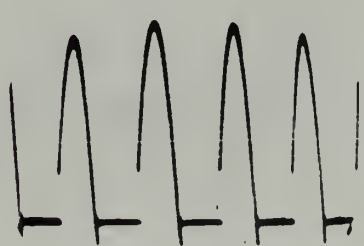

$\alpha = 140°$ $I_a = 6$ a.

FIG 5 — PLATE TO CATHODE VOLTAGE WAVEFORM

ANALOGUE

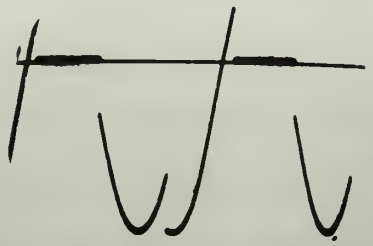

$\alpha = 50°$ $I_a = 52$ ma.

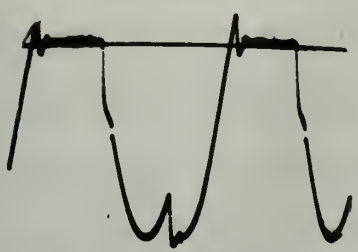

$\alpha = 50°$ $I_a = 11$ ma.

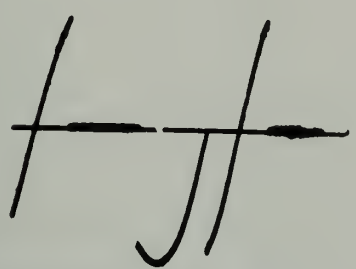

$\alpha = 90°$ $I_a = 52$ ma

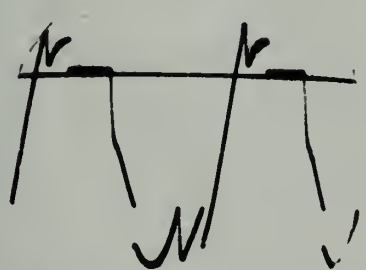

$\alpha = 90°$ $I_a = 9$ ma.

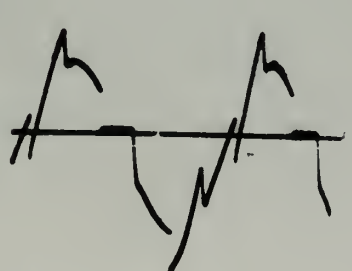

$\alpha = 140°$ $I_a = 5.7$ ma.

MOTOR

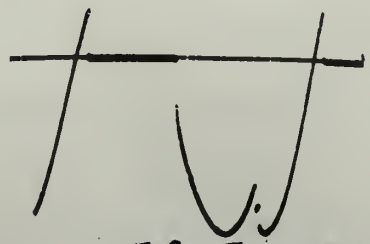

$\alpha = 50°$ $I_a = 56$ a.

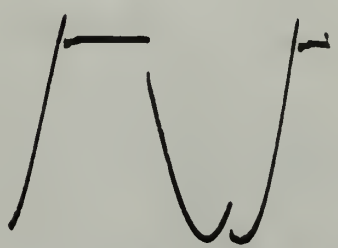

$\alpha = 50°$ $I_a = 12$ a.

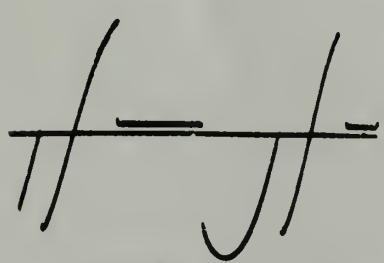

$\alpha = 90°$ $I_a = 56$ a.

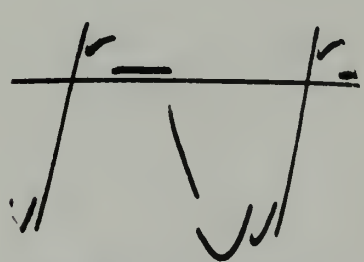

$\alpha = 90°$ $I_a = 10$ a.

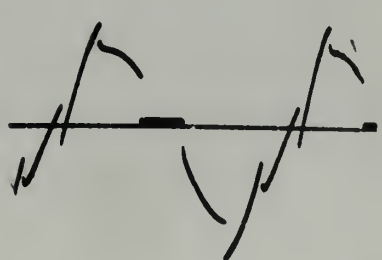

$\alpha = 140°$ $I_a = 6$ a.

mined by measuring the direct motor terminal voltage and subtracting the direct voltage drop due to the measured direct armature current. The points obtained are shown on Figure 2 reduced to a per unit basis and corrected for variations in supply voltage. These tests indicated no instability and no oscillation of the armature current when the pulses cut off during discontinuous conduction. Wave forms were photographed for this unit under conditions corresponding approximately to those used with the analogue circuit and are shown on Figures 3, 4 and 5.

mined by measuring the direct motor terminal voltage and subtracting the direct voltage drop due to the measured direct armature current. The points obtained are shown on Figure 2 reduced to a per unit basis and corrected for variations in supply voltage. These tests indicated de instability and no oscillation of the armature current when the pulses cut off during discontinuous conduction. Here forms were photographed for this unit under conditions corresponding approximately to those used with the analogue circuit and are shown on Figures 3, 4, and 5.

ANALYSIS OF ANALOGUE CIRCUIT PERFORMANCE

Wave Forms.

Comparison of the oscilloscope photographs of the wave forms of armature voltage, armature current and plate to cathode voltage of Figures 3, 4, and 5, indicates that the basic steady-state phenomena of the system are properly represented in the analogue circuit. The armature voltage wave forms for discontinuous conduction show up the major difference encountered, the behavior of the circuit when each current pulse cuts off. The cutoff transient in the current wave forms is not very apparent in these photographs, but analogue armature voltage shows the same underdamped oscillation as it returns to the average value. The similar voltage in the motor does not oscillate and indicates an overdamped behavior. The current overshoot observable on the actual ignitron pulses is probably the result of the time required for deionization. Another point of interest is the abrupt rise at the beginning of the ignitron current pulse under certain conditions which could be caused by a capacitive effect in the leads to the motor or in the housing of the motor itself.

Performance Curves.

The counter-emf versus armature current curves shown on Figure 2 for both the motor and analogue indicate fairly good correlation between the two units. The curves as actually plotted show the theoretical performance and were obtained by

ANALYSIS OF ANALOGUE CIRCUIT PERFORMANCE

Wave Forms.

Comparison of the oscillograph photographs of the wave forms of armature voltage, armature current and plate to cathode voltage of figures 3, 4, and 5, indicates that the basic steady-state phenomena of the system are properly represented in the analogue circuit. The armature voltage wave forms for discontinuous commutation show up the major difference encountered, the behavior of the circuit when each current pulse cuts off. The cutoff transient in the current wave forms is not very apparent in these photographs, but analogue armature voltage shows the same underdamped oscillation as it returns to the average value. The similar voltage in the motor does not oscillate and indicates an overdamped behavior. The current overshoot observable on the actual ignitron pulses is probably the result of the time required for deionization. Another point of interest is the abrupt rise at the beginning of the ignition current pulse under certain conditions which could be caused by a capacitive effect in the leads to the motor or in the housing of the motor itself.

Performance Curves.

The counter-emf versus armature current curves shown on Figure 2 for both the motor and analogue indicate fairly good correlation between the two units. The curves as actually plotted show the theoretical performance and were obtained by

the methods described on page 49. The experimental points for the motor and analogue show good correlation with each other and with the theoretical curves, considering the fact that the means used for setting the phase shift angles were not accurate within at least 2^{o}.

The non-linear portions of the curves at low armature currents or low voltage are the regions of discontinuous conduction while the straight-line portions to the right are for continuous conduction. The motor performance curves for which counter-emf was obtained by subtracting calculated armature voltage drop from the observed applied direct voltage are fairly flat for high currents; but if speed had been plotted directly, a rising characteristic would have been obtained because of armature reaction.

The analogue curves, on the other hand, break away from both the theoretical and actual motor curves in the boundary region between discontinuous and continuous conduction. This is especially noticeable at firing angles of 90^{o} and 110^{o}, although the condition was found to a certain degree at all angles. The operation of the circuit was actually unstable in these regions, the average current oscillating with a frequency of about 1 cycle per second by as much as 20% and the counter-emf by about 5%.

Observations of the current pulses on an oscilloscope indicated that this was caused by the current cutoff transient mentioned previously. As the load current was increased

the methods described on page 49. The experimental points for the motor and analogue show good correlation with each other and with the theoretical curves, considering the fact that the means used for setting the phase shift angles were not accurate within at least 2°.

The non-linear portions of the curves at low armature currents or low voltage are the regions of discontinuous conduction while the straight-line portions to the right are for continuous conduction. The motor performance curves for which counter-emf was obtained by subtracting calculated armature voltage drop from the observed applied direct voltage are fairly flat for high currents; but if speed had been plotted directly, a rising characteristic would have been obtained because of armature reaction.

The analogue curves, on the other hand, break away from both the theoretical and actual motor curves in the boundary region between discontinuous and continuous conduction. This is especially noticeable at firing angles of 90° and 120°, although the condition was found to a certain degree at all angles. The operation of the circuit was actually unstable in these regions, the average current oscillating with a frequency of about 1 cycle per second by as much as 20% and the counter-emf by about 5%.

Observations of the current pulses on an oscilloscope indicated that this was caused by the current cutoff transient mentioned previously. As the load current was increased

gradually during discontinuous conduction, the start of a current pulse would break abruptly between peaks of the cutoff transient from the preceding pulse. For a load at which the pulse first broke away, both conditions were unstable and the pulse initiation would break back and forth between the two peaks as shown in Figure 6 (a) resulting in average current oscillations in the circuit. With further increase in loading, oscillations ceased with the pulse originating from a peak of the transient as shown by Figure 6 (b); but this condition resulted in the offset points on the performance curves. At a slightly higher load, the break occurred as indicated in Figure 6 (c), again causing oscillations in the circuit until the load was sufficient to give full continuous conduction.

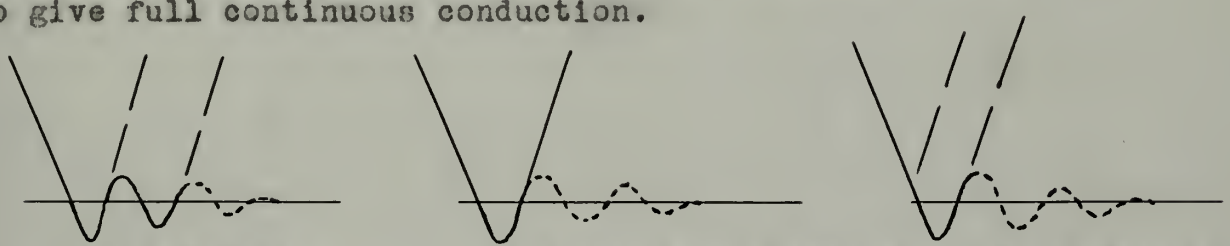

(a) Unstable (b) Stable but offset (c) Unstable

Figure 6. Current Pulses with Unstable Operation

Transient Response.

Comparison of the transient speed response times for step changes in firing angle given in Table II for the motor and analogue indicate that the analogue has the same general dynamic characteristic as the actual motor. However, it is obvious that any simulated conditions involving operation in or through regions where the steady-state characteristics of the two differ will not yield reliable results.

gradually during discontinuous conduction, the start of a current pulse would break abruptly between peaks of the cutoff transient from the preceding pulse. For a load at which the pulse first broke away, both conditions were unstable and the pulse initiation would break back and forth between the two peaks as shown in Figure 6 (a) resulting in sustained current oscillations in the circuit. With further increase in loading, oscillations ceased with the pulse originating from a peak of the transient as shown by Figure 6 (b); but this condition resulted in the offset points on the performance curves. At a slightly higher load, the break occurred as indicated in Figure 6 (c), again creating oscillations in the circuit until the load was sufficient to give full continuous conduction.

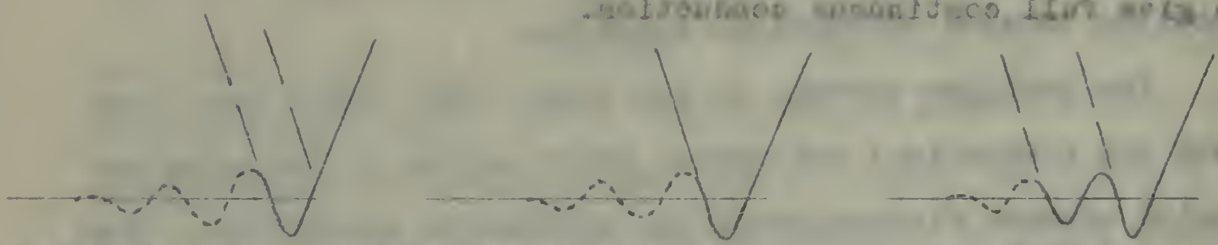

(a) Unstable (b) Stable but offset (c) Unstable

Figure 6. Current Pulses with Unstable Operation

<u>Transient Response.</u>

Comparison of the transient speed response times for step changes in firing angle given in Table II for the motor and analogue indicate that the analogue has the same general dynamic characteristics as the actual motor. However, it is obvious that any simulated conditions involving operation in or through regions where the steady-state characteristics of the two differ will not yield reliable results.

Elimination of Current Cutoff Transient.

From the previous discussion, it is apparent that the major difficulty in the operation of the analogue circuit was the current pulse cutoff transient during discontinuous conduction. From an analysis of the circuit it is evident that when the current decreases to zero and conduction through the rectifier ceases almost instantaneously, the energy stored in the inductance unit is released as a voltage impulse. Since the non-conducting rectifier acts as an open switch, current will flow in the circuit as seen by the inductance only if some path for it exists around the rectifier. Such a path could be provided by the following factors:

a) stray wiring capacitance in the circuit,

b) interelectrode capacitance in the thyratrons,

c) capacitance between the anode transformer secondary windings and ground.

Since all auxilliary equipment such as the phase shift transformer and the thyratron heater transformers were connected to the grounded cathode any capacitance to ground of these units would not be effective.

Removing two of the three thyratrons from the circuit to reduce the effective interelectrode capacitance produced no observable affect on the transient. Mercury vapor type tubes (FG-17) were also substituted with no improvement. By breaking the connection between cathode and ground, however, the amplitude of the transient was reduced appreciably, indicating that the major effects were caused by capacitance

Elimination of Current Crowding.

From the foregoing discussion, it is apparent that the major difficulty in the operation of the multiple gate gate-controlled thyristor was the current crowding resulting from nonuniform conduction. This is analyzed in the regions that when the current gain becomes unity, the energy stored in the semiconductor must be removed in a voltage dependent manner. Since the gate-controlled rectifier does not open until only it some part of the current will be shunted around the junction. Such a part could be provided by the following features:

a) extra gating contacts in the circuit,

b) interelectrode capacitance in the thyristor,

c) additional external circuit elements.

Since all auxiliary components used as the phase split network and clamps.

Because the effects of the three phenomena just mentioned to impose the effective interconnected combinations produced do appear unlikely that the thyristor will not be effective.

[20-13] were also employed with no improvement. In these- the capacitance between gates and ground, however, operation at the frequency was reduced appreciably, while the current gain was increased [20-14].

to ground of some point between the inductance and the plates of the thyratrons around the lower portion of the circuit as shown in Figure 1. Since the anode transformer cases were not grounded, the most probable cause of the trouble was the interwinding capacitance of these transformers; inasmuch as the primaries provided a path to ground through the power system. The actual capacitance in the transformers was probably of the same order of magnitude as that in the transformers used with the ignitron rectifier; but because of the scaled down parameters of the analogue circuit, its effect was magnified a thousand times.

Smaller heater type transformers were tried in place of the large anode transformers, but no appreciable difference was noted. These and the large transformers were connected in zig-zag instead of delta-wye, also causing no improvement.

It was found that with a 50,000 ohm resistor in the ground connection the transient was damped out in the minimum time, although its peak amplitude was somewhat greater than with the ground circuit open. This arrangement was used for all the tests.

After the analogue circuit was disassembled, it was found that on the actual ignitron rectifier a 2000 ohm resistor was permanently installed directly across the line connected to the d-c output. A corresponding resistor was not tried in the analogue circuit, but it is probable that it would have about the same effect as the resistor in the ground connection.

Determination of the Equivalent Armature Resistance.

One of the problems involved in setting up the analogue circuit is the determination of the equivalent armature resistance of the motor. The resistance unit used in the analogue circuit had the same d-c and a-c resistance up to 1000 cps. However, the measured 60 cycle a-c resistance of the actual motor was more than twice the measured d-c resistance. The 60 cycle a-c resistance of the motor was used in determining the equivalent for the analogue circuit; and although no justification for this can be found, the correspondence of the actual performance curves with the theoretical and analogue curves indicates that this gives better results than if the d-c resistance had been used.

EVALUATION OF THE ANALOGUE CIRCUIT

The evaluation of the analogue circuit may be broken down into two aspects according to the use for which it is intended; first for obtaining the steady-state speed (counter-emf) versus armature current characteristics, and second, for transient investigations involving the use of feedback.

Steady-State.

Even though the basic steady-state phenomena of the system are properly represented in the analogue circuit, the performance curves are not accurate in the boundary region between discontinuous and continuous conduction as explained in the previous section. Since these inaccuracies cover a considerable portion of the overall curves, and since it does not appear possible to completely eliminate the current oscillations which cause them, the analogue circuit is not considered practicable for obtaining complete accurate steady-state performance data.

Transient.

The analogue circuit may be useful, however, for transient investigations not requiring precise correspondence in the regions where the characteristics are inaccurate or the operation unstable. The important area for transient investigation using feedback appears to be the problem of improving the slowdown characteristics. Another field for investigation is the stabilization of speed with change in load. It is considered practicable to use the analogue

The simulation of the analogue circuit may be carried down into two stages according to the use for which it is intended; first for obtaining the steady-state speed (constant) versus armature current characteristics, and second, for transient investigations involving the use of Laplace.

Steady-State.

Even though the basic steady-state phenomena of the system are fairly straightforward in the analogue circuit, the performance curves are not accurate in the boundary region between discontinuous and continuous commutation as explained in the previous section. Since these inaccuracies cover a considerable portion of the steady curves, and since it does not appear possible to completely eliminate the current oscillations which cause them, the analogue is not considered practicable for obtaining complete accurate steady-state performance data.

Transient.

The analogue circuit may be useful, however, for transient investigations not requiring precise information in the region where the characteristics are inaccurate or the operation unstable. The important item for transient investigation using feedback systems is the problem of improving the dynamic characteristics. Another field for

circuit for investigations along either of these lines. However, any feedback work involving stability will be complicated by the inherent instability of the analogue circuit in certain regions.

ANALYTICAL PREDICTION OF TRANSIENT RESPONSE

An analysis of the equivalent circuit of the d-c machine and its load together with performance curves for the ignitron-motor combination leads to a relatively simple means of predicting the transient response of the system for changes in firing angle or load without resorting to actual experiment.

Equivalent Circuit.

As previously discussed, a separately excited d-c machine and its load may be represented by the equivalent circuit of Figure 7.

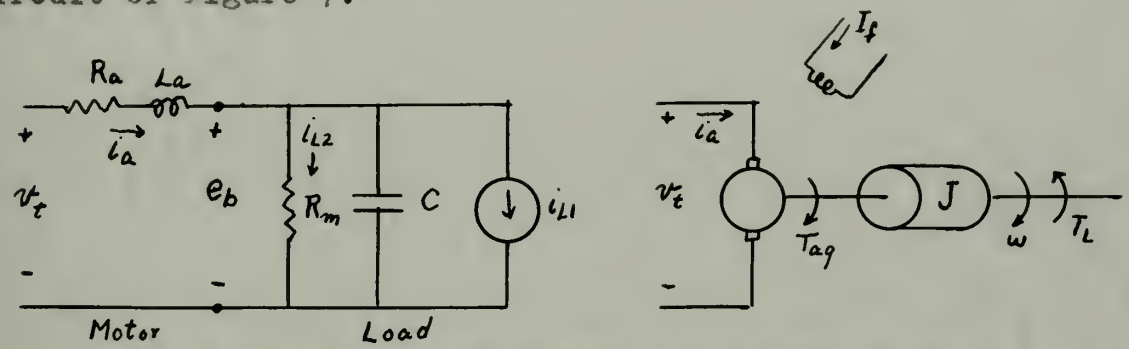

Figure 7. D-C Motor and Equivalent Circuit.

For I_f constant $\quad T_{ag} = Ki_a \qquad (9)$

$$J = K^2C \qquad (10)$$

$$E_b = Kw \qquad (11)$$

$$T_{L1} = Ki_{L1} \qquad (12)$$

$$T_{L2} = Ki_{L2} = \frac{E_b}{KR_m} = \frac{K^2w}{R_m} \qquad (13)$$

For a linear analysis i_{L1} and R_m are constant if the machine is running, simulating a load with a component of constant torque and a component that is directly proportional to speed. Using mks units $k_1 = k_2 = K$.

ANALYTICAL PREDICTION OF TRANSIENT RESPONSE

An analysis of the equivalent circuit of the d-c machine and its load together with performance curves for the ignitron-motor combination leads to a relatively simple means of predicting the transient response of the system for changes in firing angle or load without resorting to actual experiment.

Equivalent Circuit.

As previously discussed, a separately excited d-c machine and its load may be represented by the equivalent circuit of Figure 7.

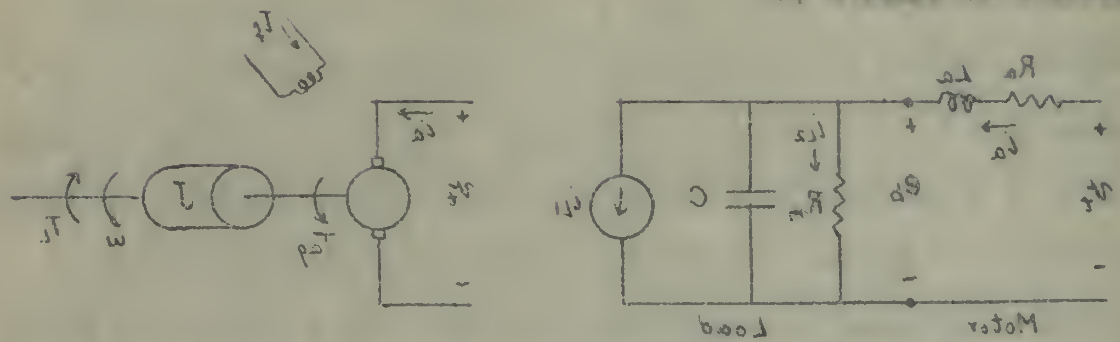

Figure 7. D-C Motor and Equivalent Circuit.

For I_f constant $\quad T_{eg} = Ki_a \quad$ (9)

$$E = K\omega \quad (10)$$

$$E_b = Ke \quad (11)$$

$$T_{L1} = Ki_{L1} \quad (12)$$

$$T_{L2} = Ki_{R_m} = \frac{Ke_b}{R_m} = \frac{K^2\omega}{R_m} \quad (13)$$

For a linear analysis i_{L1} and R_m are constant if the machine is running, simulating a load with a component of constant torque and a component which is directly proportional to speed. Using mks units $K_1 = K_2 = K$.

Steady-State Analysis.

The steady-state speed-torque curves for such a motor with various values of terminal voltage are as shown in Figure 8, and are derived from the relationship

$$E_b = V_t - i_a R_a \tag{14}$$

$$\text{or} \qquad w = \frac{V_t}{K} - \frac{R_a}{K^2} T_{ag} \tag{15}$$

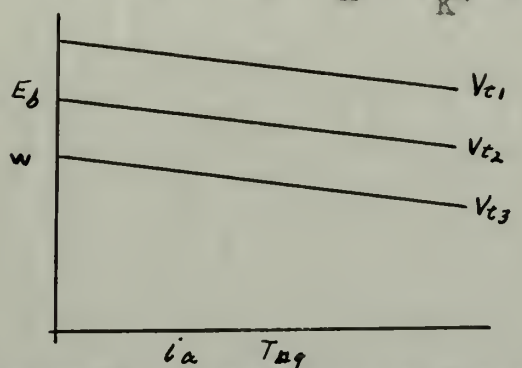

Figure 8. Speed-Torque Characteristics for Separately Excited D-C Motor.

The slope of these lines is

$$\frac{\delta E_b}{\delta i_a} = -R_a \tag{16}$$

$$\text{or} \qquad \frac{\delta w}{\delta T_m} = \frac{R_a}{-K^2} \tag{17}$$

If a particular load characteristic is plotted on the same coordinates, it is a straight line as shown in Figure 9 with the horizontal axis intercept of i_{L1} or T_{L1} and slopes

$$\frac{\delta E_b}{\delta i_L} = R_m \tag{18}$$

$$\frac{\delta w}{\delta T_L} = \frac{R_m}{K^2} \tag{19}$$

Power-Speed Relation:

The steady-state speed-torque curves for both a motor with torque values of constant voltage are as shown in Figure 8, and are derived from the relationship

$$T_D = T_E - \frac{1}{2} \beta \omega \tag{12}$$

or $$\omega = \frac{T_E}{\frac{\beta}{2}} - \frac{T_D}{\frac{\beta}{2}} \tag{13}$$

Figure 8. Speed-Torque Characteristics for Separately Excited D-C Motor.

The slope of above lines is

$$\frac{\partial \omega}{\partial T_E} = -\frac{1}{\frac{\beta}{2}} \tag{14}$$

or $$\frac{\partial T_E}{\partial \omega} = -\frac{\beta}{2} \tag{15}$$

If a particular load characteristic is plotted on the same coordinates, it is a straight line as shown in figure 9 with the horizontal axis intercepts of T_T or T_L and having

$$\frac{\partial T_D}{\partial \omega} = \frac{\beta}{2} \tag{16}$$

$$\frac{\partial \omega}{\partial T_D} = \frac{2}{\beta} \tag{17}$$

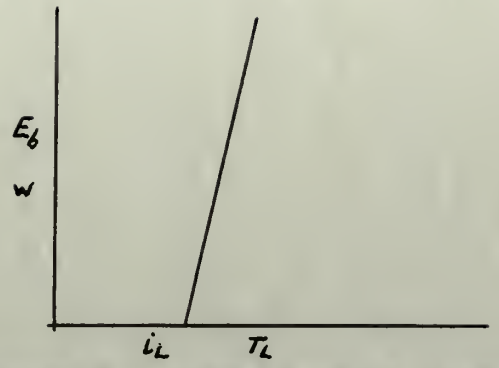

$$T_L = T_{L1} + T_{L2}$$

$$i_L = i_{L1} + i_{L2}$$

Figure 9. Speed-torque Characteristics of Load.

The steady-state operating conditions for a particular load and terminal voltage are given by the intersection of the load and motor speed-torque curves.

This same reasoning may be applied to the ignitron-motor combination to determine the steady-state operating conditions. In this case, however, the motor speed-torque curves are not straight lines but are similar to Figure 2, and are plotted for firing angle as a parameter rather than applied terminal voltage.

Transient Analysis.

The transient of primary interest is the behavior of motor speed for a change in firing angle. The transient analysis is most easily performed by considering the electrical equivalent circuit of Figure 7 rather than the mechanical system. The electro-mechanical conversion factor, K, is a constant if armature reaction is neglected or assumed constant, permitting a conversion at any stage of the analysis from electrical to mechanical parameters.

The armature inductance will be neglected since, for most integral horsepower motors used in power applications,

Figure 5. Speed-torque characteristics of load.

The steady-state operating conditions for a particular load and terminal voltage are given by the intersection of the load and motor speed-torque curves.

This same reasoning may be applied to the induction-motor connection to determine the steady-state operating conditions. In this case, however, the motor speed-torque curves are not straight lines but are similar to figure 5, and are plotted for fixed values of the parameter rotor current applied terminal voltage.

Transient analysis.

The treatment of primary interest in the behavior of motor speed for a change in fixed angle. The standard analysis is made easily tractable by considering the sinusoidal equivalent circuit of figure 3 rather than the exact circuit system. The steady-state sinusoidal conversion factor, k, is a constant if armature reaction is neglected or assumed constant, partially compensated or corrected. If any analysis time discretion to excitation parameters.

The armature inductance will be neglected since, for most integral horsepower motors used in power applications,

its effect is negligible in comparison with the effect of the motor and load inertia or its equivalent capacitance. Furthermore, under conditions of discontinuous conduction through the ignitron rectifier, there is no current flowing in the armature circuit during a portion of each cycle and no net energy is stored in the inductance from cycle to cycle; consequently the speed transient is not affected by the inductance under these circumstances. With continuous conduction, the inductance may be effective; but, as will be brought out subsequently, the transient performance of the motor under these conditions is not affected by the rectifier and presents no new problems.

With the armature inductance omitted, the circuit of Figure 7 may be converted into an equivalent as shown in Figure 10.

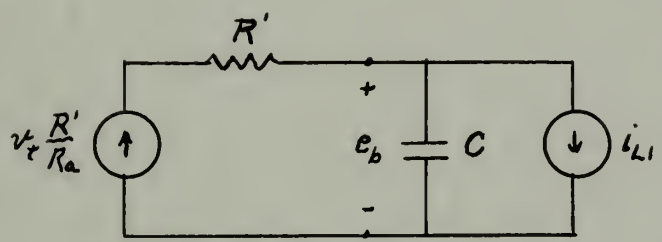

$$R' = \frac{R_a R_m}{R_a + R_m}$$

Figure 10. Equivalent Circuit for D-C Motor and Load.

The Kirchhoff equations for this circuit are

$$v_t \frac{R'}{R_a} = i_a' R' + e_b \qquad (20)$$

$$i_a' = i_{L1} + C \frac{de_b}{dt} \qquad (21)$$

$$v_t \frac{R'}{R_a} - R' i_{L1} = R' C \frac{de_b}{dt} + e_b \qquad (22)$$

Figure 10. Equivalent circuit for R-C motor and load.

For a step change in either v_t or i_{L1}

$$e_b = E_{bi} + (E_{bf} - E_{bi})\left(1 - \varepsilon^{-\frac{t}{R'C}}\right) \qquad (23)$$

where E_{bi} = initial E_b corresponding to initial speed

E_{bf} = final E_b corresponding to final steady-state speed

To apply this result to the ignitron-motor combination it is necessary to determine the values of Ra, Rm, E_{bi} and E_{bf} to be used. These will be arrived at by investigating the actual behavior of the circuit or motor during the transient.

Considering first the performance of the d-c motor with speed-torque characteristics as in Figure 8 for a step change in terminal voltage, the sequence of events is as shown in Figure 11 as follows.

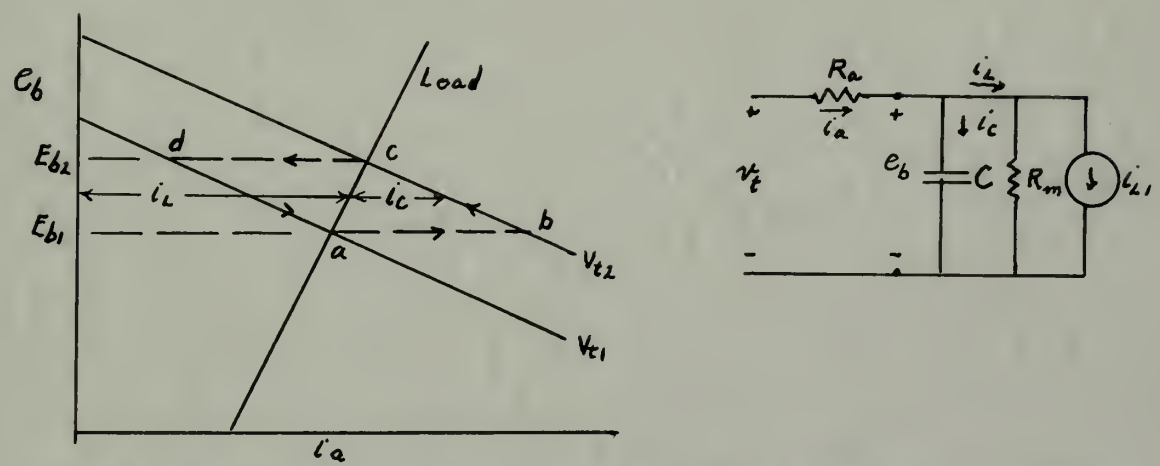

Figure 11. D-C Motor Performance for Speed Transient.

The initial conditions for the given load and terminal voltage V_{t1} are given by the steady-state operating point at a with $e_b = E_{b1}$ and $i_a = i_L$.

Figure 12. E-C model representation for diode transient.

The initial conditions for the given load and terminal voltage V_{cl} are given by the steady-state operating point a with $e_b = E_{bb}$ and $i_b = I_b$.

At t = 0 the terminal voltage is changed to V_{t2}, and at t = 0+ the operating point has moved horizontally to point b, since the charge on the condenser and hence e_b cannot change instantaneously. For t > 0 the charging current to the condenser ($i_c = i_a - i_L$) is given by the horizontal distance between the motor curve and load curve; and as the condenser charges, e_b increases so that the motor operating points move along the line b-c until the final steady-state condition is reached at point c.

Similarly, if the initial conditions are taken at point c, and the terminal voltage is reduced from V_{t2} to V_{t1}, the operating point moves to point d at t = 0+. In this case for t > 0, i_c is negative since i_a is less than i_L, and the charge on the condenser is reduced, decreasing e_b along the curve d-a until the final steady condition at point a is reached.

This reasoning may be clearer if applied to the mechanical operation of the motor. If a step change is made in the terminal voltage, the speed and hence the back-emf cannot change instantaneously because of the load (or rotor) inertia. The armature current increases almost instantaneously, however, to $\frac{V_{t2} - E_{b1}}{R_a}$ and produces an air gap torque T_{ag} which provides the load torque, T_L, and an accelerating torque, T_a. As the rotor accelerates, the speed and back-emf increase and i_a and T_{ag} decrease until the new steady state condition is reached. The detailed analysis of the electrical

equivalent may be applied to the mechanical case by taking $T_m = Ki_a$, $T_L = Ki_c$ and the speed equal to e_b/K.

For the non-linear performance curves of the ignitron-motor combination a similar analysis may be carried out for a change in firing angle as shown in Figure 12.

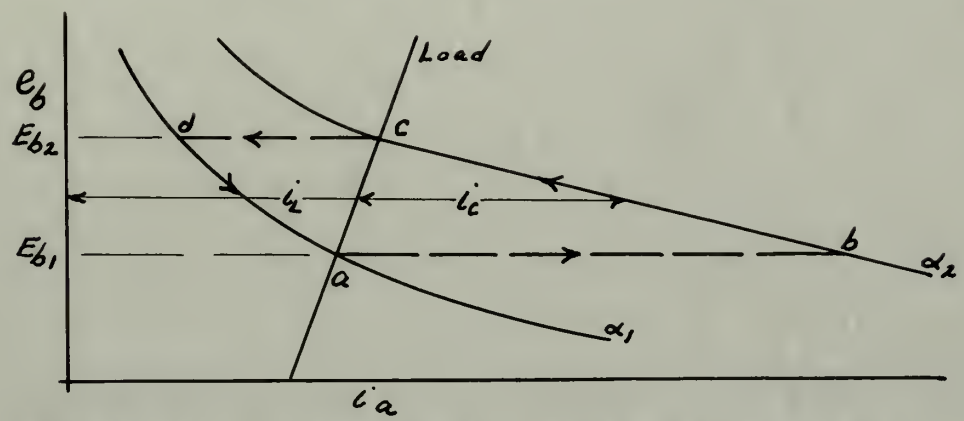

Figure 12. Ignitron-motor System Performance for Speed Transient.

For a step change in firing angle from α_1 to α_2 the output shifts from point a to point b at t = 0+ and for t > 0 moves along the α_2 curve from b to c until the final steady-state condition at c is reached. Similarly for a change from α_2 to α_1, the output moves from point c to point d at t = 0+ and then moves along the α_1 curve until the steady-state condition at a is reached.

To determine the appropriate values of E_{bi}, E_{bf}, R_a and R_m for the ignitron-motor system necessary for obtaining the analytical expression for the transient performance of e_b given by equation (23), it is only necessary to compare the linear d-c motor and non-linear ignitron motor curves of Figures 11 and 12. In Figure 11, R_a is the nega-

Figure 12. Limiting-curve diagram for open-ended transmission line.

tive slope of the V_{t1} and V_{t2} curves along which the motor output moves during the transient. By analogy, R_a in Figure 12 is the negative slope of the curves c-b and d-a and is different for the conditions of increasing and decreasing speed. In both cases, however, R_m is the slope of the load characteristic and E_{bi} and E_{bf} are the values of e_b at $t = 0+$ (point b or d) and $t = \infty$ (point c or a).

Summary.

The speed transients for the ignitron-motor system for a step change in firing angle can thus be predicted by use of the electrical performance curves for the combination. The procedure is summarized as follows:

a) Plot on the ignitron-motor curves the electrical equivalent of the load speed-torque curve. This curve need not be a straight line.

b) For the initial and final firing angle α_i and α_f, read off E_{bi} and E_{bf}.

c) Determine R_a from the average slope of the α_f curve between the points where $e_b = E_{bi}$ and $e_b = E_{bf}$. $(R_a = -\frac{\delta e_b}{\delta i_a})$.

d) Determine R_m from the average slope of the load curve between the points where $e_b = E_{bi}$ and $e_b = E_{bf}$. $(R_m = \frac{\delta e_b}{\delta i_L})$.

e) Knowing the electrical equivalent of the inertia $C = \frac{J}{K^2}$, find the time constant for this condition.

$$\tau = \frac{R_a R_m}{R_a + R_m} \times C \qquad (24)$$

f) The transient for E_b is then given by

$$Kw = e_b = E_{bi} + (E_{bf} - E_{bi})(1 - \varepsilon^{-t/\tau}) \quad (25)$$

The speed transient for a step change in load can be predicted using the above procedure modified in the following respects:

a) Initial and final load speed-torque curves are plotted.

b) E_{bi} and E_{bf} are found from the two load curves and the given firing angle curve.

c) R_m is determined from the slope of the final load curve.

Special Conditions.

For certain situations using the above procedures, the slope along either curve may change radically during the course of the transient as illustrated in Figure 13. In these instances the speed transient may be broken down into two or more successive portions, each portion characterized by a time constant (equation (24)) obtained from the slopes of straight line approximations to the motor and load curves, and with E_{bf} determined from the intersection of the two assumed straight lines starting at E_{bi} on the two curves. When e_b reaches a value where the curve slopes change appreciably for the succeeding portion of the transient, new straight line approximations are made for determining a new time constant and E_{bf} as before, but for this portion E_{bi} is taken as the value of e_b at which the first portion of the transient was terminated.

transient was terminated.

taken as the value of e^2 at which the first portion of the time constant and P^{01} as before, but for this portion P^{02} is neglected using the above procedure modified in the following respects:

f) The transient for P is then given by

$$P = e^{P} = P_{f1} + (P_{0f} - P_{01})(1 - e^{-t/\tau}) \quad (13)$$

The speed transient for a step change in load can be predicted using the above procedure modified in the following respects:

a) Initial and final speed-torque curves are plotted.

b) E^{01} and P^{01} are found from the two load curves and the given firing delta curve.

c) P^{02} is determined from the slope of the first load curve.

Special Conditions.

For certain situations using the above procedure, the slope along either curve may change radically during the course of the transient as illustrated in Figure 23. In these instances the speed transient may be broken down into two or more successive portions, each portion characterized by a time constant (equation (11)) obtained from the slopes of straight line approximations to the curve and load curve, and with P^{01} determined from the intersection of two assumed straight lines operating at P^{02} on the two curves. Then e^{P} becomes a value where the curve slopes change- ably for the successive portion of the transient, new straight line approximations are made for determining a new time constant and P^{01} as before, but for this portion P^{02} is

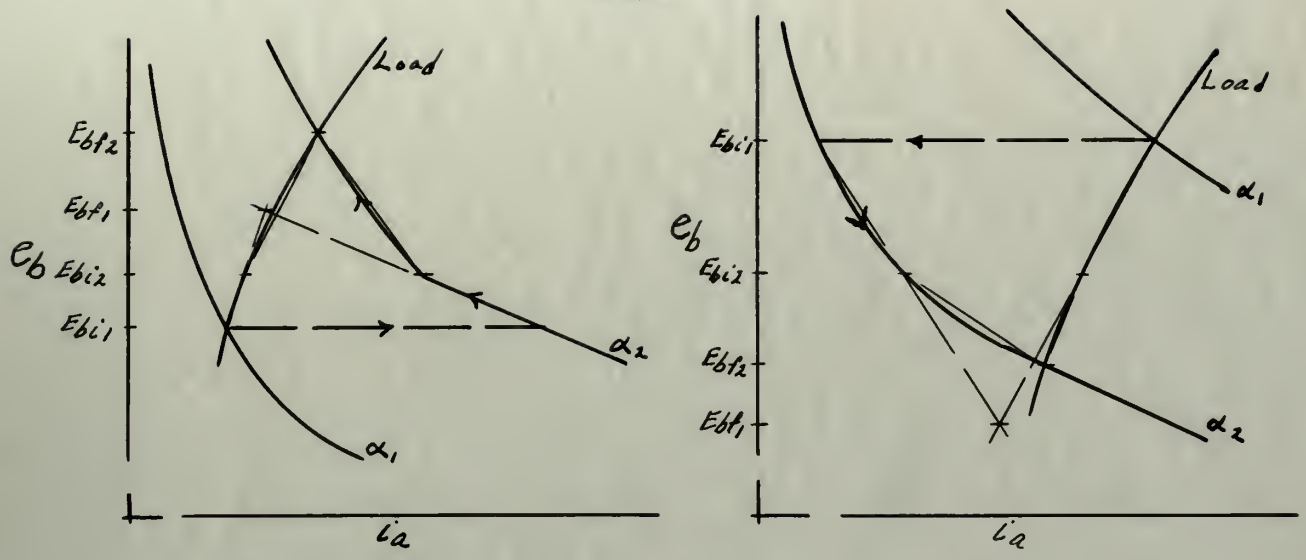

Figure 13. Transients With Change of Slope.

The speed transient for either condition of Figure 13 and a step change in firing angle from α_1 to α_2 is given by

$$e_b = E_{bil} + (E_{bf_1} - E_{bi_1})\ (1 - \varepsilon^{-t/\tau_1}) \qquad (25a)$$

for $0 < t < t_1$

$$\tau_1 = \frac{R_{a1}R_{m1}}{R_{a1}+R_{m1}} \times C \qquad (24a)$$

$$e_b = E_{bi_2} + (E_{bf_2} - E_{bi_2})\ (1 - \varepsilon^{-t/\tau_2}) \qquad (25b)$$

for $t > t_1$

$$\tau_2 = \frac{R_{a2}R_{m2}}{R_{a_2}+R_{m_2}} \times C \qquad (24b)$$

where t_1 is the value of t for which e_b of equation (25a) equals E_{bi_2}.

This same line of reasoning may be applied in finding the transient speed response to any arbitrary input by a step by step method or even to a sinusoidal input if the operating output is plotted point by point on the perform-

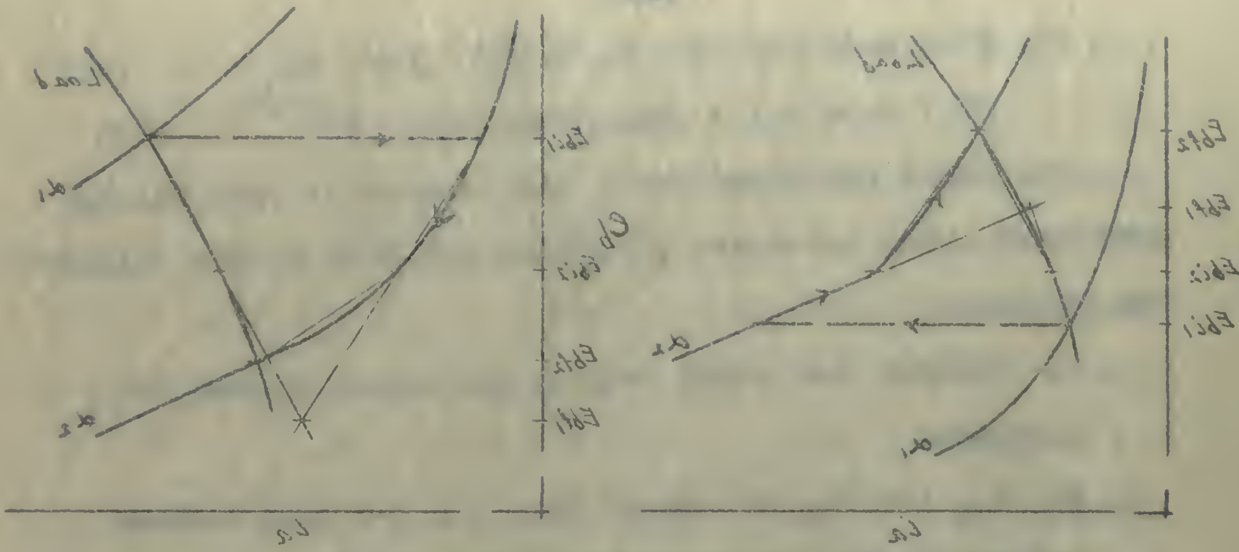

Figure 13. Transients with Change of Slope.

The speed transient for either condition of Figure 13 and a step change in firing angle from α_1 to α_2 is given by

$$e_b = E_{bi1} + (E_{bf1} - E_{bi1})(1 - \epsilon^{-t/\tau_1}) \qquad (23a)$$

for $0 < t < t_1$

$$\tau_1 = \frac{R_1 R_{m1}}{R_1 + R_{m1}} \times C \qquad (23b)$$

$$e_b = E_{bi2} + (E_{bf2} - E_{bi2})(1 - \epsilon^{-t/\tau_2}) \qquad (23c)$$

for $t > t_1$

$$\tau_2 = \frac{R_2 R_{m2}}{R_2 + R_{m2}} \times C \qquad (23d)$$

where t_1 is the value of t for which e_b of equation (23a) equals E_{bi2}.

This same line of reasoning may be applied in finding the transient speed response to any arbitrary input by a step by step method or even to a sinusoidal input if the operating output is plotted point by point as was perform-

ance curves and the proper values are used for the time constant and forcing function. In general, however, the three-phase ignitron-motor performance for large disturbances is very non-linear, and no simple transfer function relating dynamic output to input can be derived for it.

Current Transients.

If an analysis for the average armature current transient is carried out similar to the above presentation, it will be found that the equation is similar in form to equation (25) and is characterized by the same time constant, equation (24). The current transient is given by

$$i_a = I_{ai} + (I_{af} - I_{ai})\,(1 - \varepsilon^{-t/\tau}) \qquad (26)$$

for $t > 0$

where $I_{ai} = i_a$ at $t = 0+$

All subscripts have the same meaning as in equations (24) and (25) as indicated on Figure 12 for the voltage transient, and the value of τ is determined in the same manner.

same curves and the proper values are used for the time constant and forcing function. In general, however, the three-phase ignitron-motor performance for large disturbances is very non-linear, and no simple transfer function relating dynamic output to input can be derived for it.

Current Transients.

If an analysis for the average armature current transient is carried out similar to the above presentation, it will be found that the equation is similar in form to equation (25) and is characterized by the same time constant, equation (24). The current transient is given by

$$i_a = I_{ai} + (I_{af} - I_{ai})(1 - \varepsilon^{-t/\tau}) \qquad (28)$$

for $t > 0$

where $I_{ai} = I_a$ at $t = 0+$

All subscripts have the same meaning as in equations (24) and (25) as indicated on Figure 12 for the voltage transient, and the value of τ is determined in the same manner.

COMPARISON OF EXPERIMENTAL AND PREDICTED SPEED TRANSIENTS

The analytical method for predicting speed transients described in the previous section was used to obtain the theoretical response curves of Figures 14 to 18 for the motor and operating conditions used in Heller's investigation.[4] These are compared with the experimental response curves which he obtained from oscillograph data, and show very close agreement in nearly all instances.

The speed-torque (counter-emf versus armature current) curves used were those of Figure 2 obtained for the ignitron-motor combination as described on page 49. The actual operating conditions[4] and the values of R_a derived from the performance curves together with the calculated time constant used for determining the theoretical transient response for the various runs are shown in Table III. The method of plotting the response in two parts with different time constants was used only for runs P-1 and J-2. Additional accuracy could be obtained by dividing some of the other transients up in the same manner, but the results as they stand are considered sufficiently accurate for engineering work.

This method of predicting transients is considered to be more satisfactory than either the full scale tests or tests with an analogue circuit. Furthermore, it points up the limitations of the ignitron-motor combination in terms of the physical parameters of the system. The major difficulty

[illegible]

The simplified method for predicting speed transients described in the previous section was used to obtain the theoretical response curves of figures 14 to 22 for the motor and operating conditions used in Kalina's investigation.

These are compared with the experimental response curves which he obtained from oscillograph data, and show very close agreement in nearly all instances.

The speed-torque (counter-emf versus armature current) curves used were those of figure 6 obtained for the generator-motor combination as described on page 49. The actual operating conditions and the values of R_a derived from the performance curves together with the calculated time constant used for determining the theoretical transient response for the various runs are given in Table III. The method of plotting the response in two parts with different time constants was used only for runs 7-1 and 7-2. Additional accuracy could be obtained by dividing some of the other transients up in the same manner, but the results as they stand are considered sufficiently accurate for engineering work.

This method of predicting transients is considered to be more satisfactory than either the full scale tests or tests with an analogous circuit. Furthermore, it points up the limitations of the generator-motor combination in terms of the physical parameters of the system. The major difficulty

in using this method is the problem of obtaining the basic counter-emf versus armature current performance curves. These curves may be obtained analytically, however, without actual tests on the system as will be described in the following section.

to swing into action in the event of obtaining the peak
conductance values mentioned earlier. However, although
these curves may be obtained qualitatively, however, without
actual knowledge of the values it will be impossible in the
following analysis.

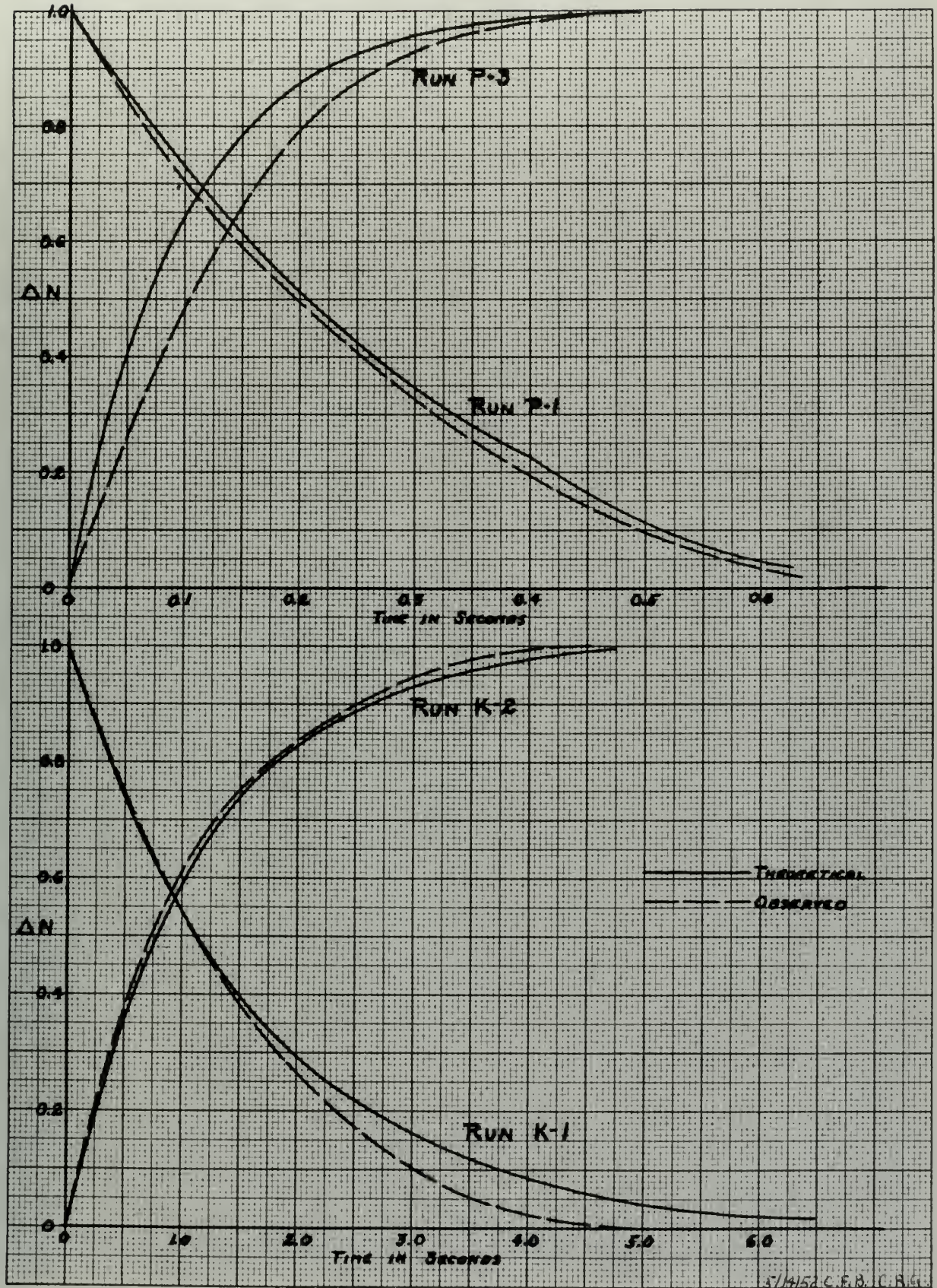

SPEED TRANSIENT FOR STEP CHANGE IN FIRING ANGLE
IGNITRON MOTOR CONTROL

FIG 14

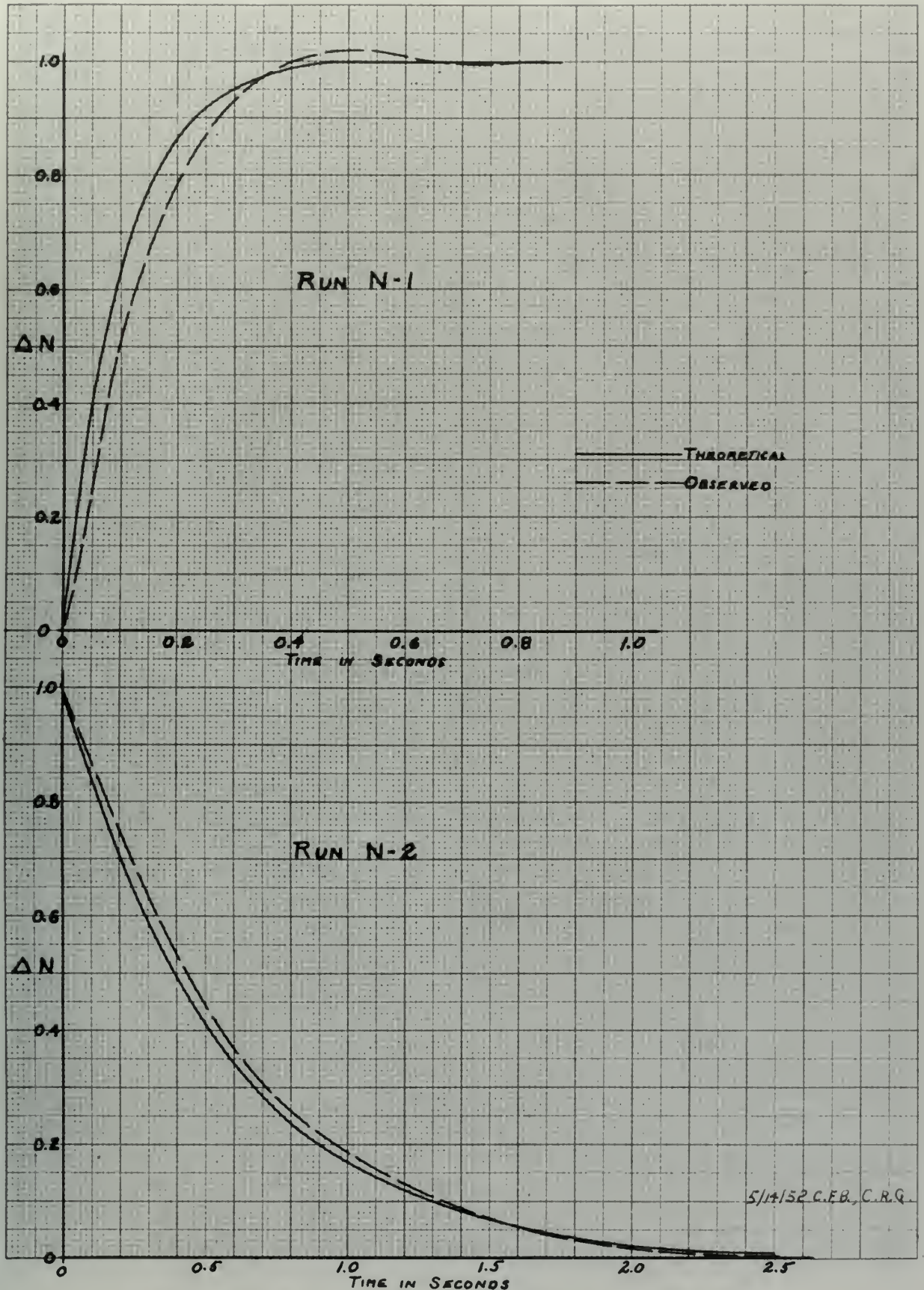

SPEED TRANSIENT FOR STEP CHANGE IN FIRING ANGLE

IGNITRON MOTOR CONTROL

FIG 15

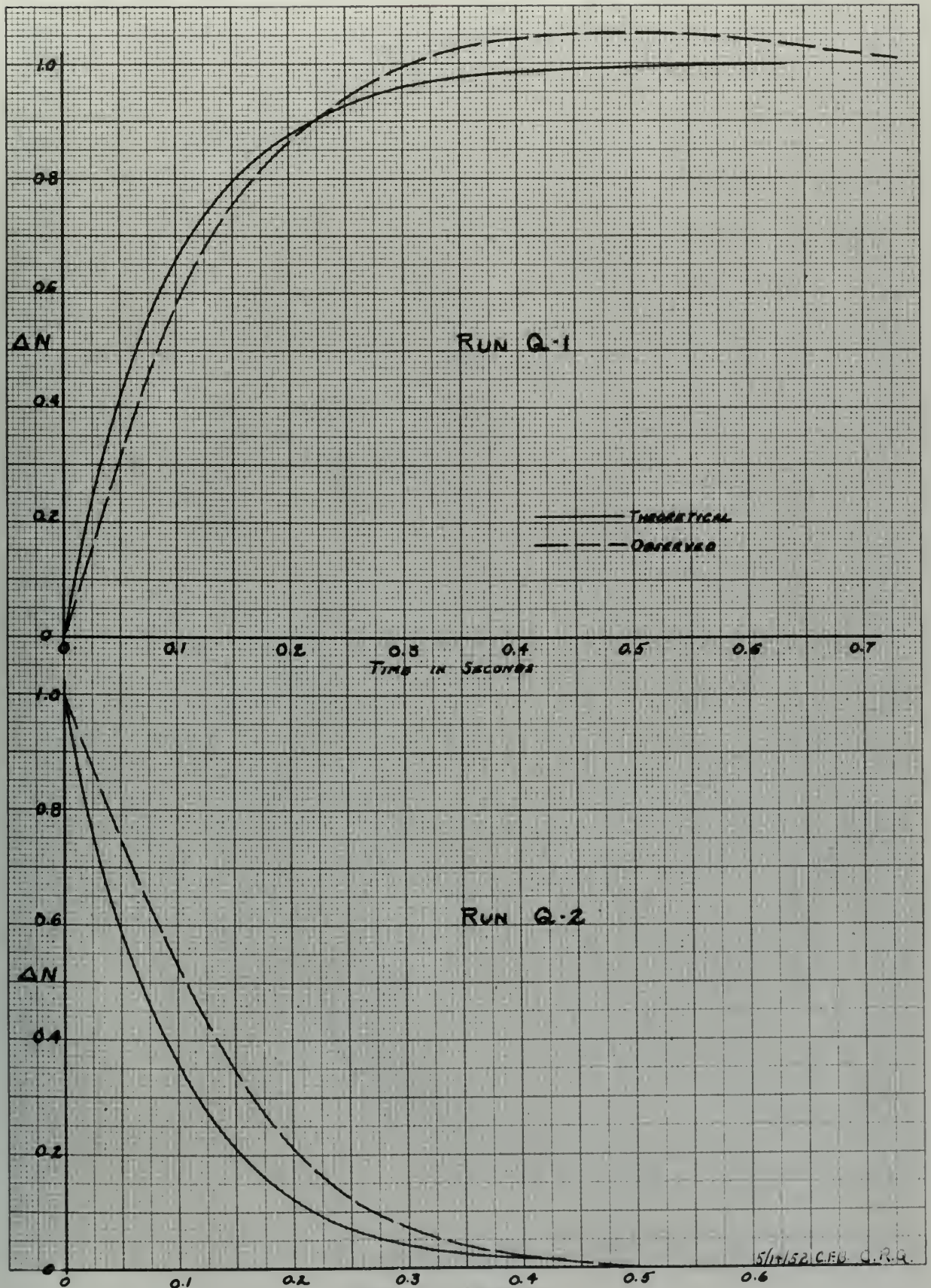

SPEED TRANSIENT FOR STEP CHANGE IN FIRING ANGLE
IGNITRON MOTOR CONTROL

FIG 16

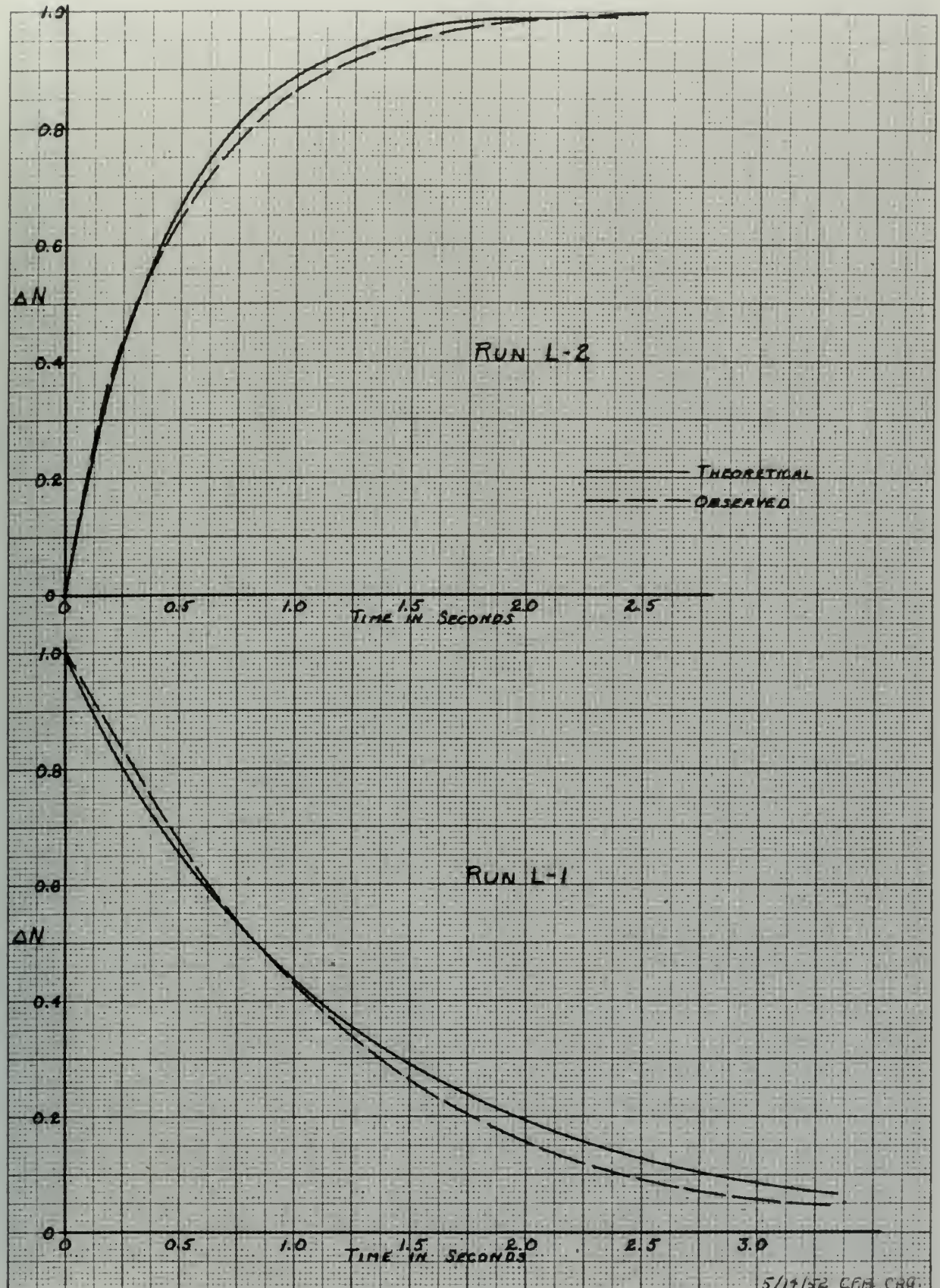

SPEED TRANSIENT FOR STEP CHANGE IN FIRING ANGLE
IGNITRON MOTOR CONTROL

FIG 17

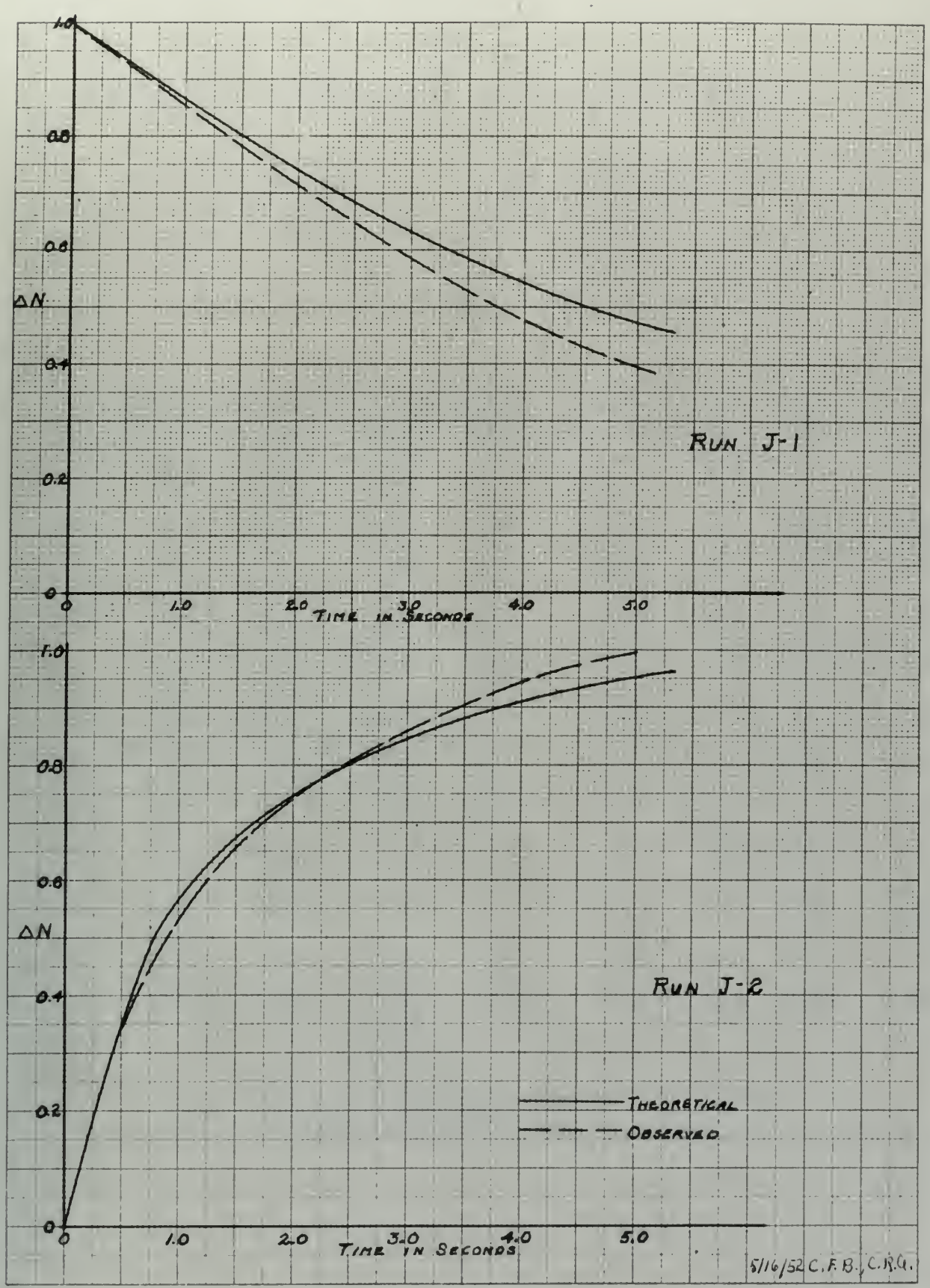

SPEED TRANSIENT FOR STEP CHANGE IN FIRING ANGLE
IGNITRON MOTOR CONTROL

FIG 18

TABLE III

OPERATING CONDITIONS AND CIRCUIT PARAMETERS FOR OBSERVED AND PREDICTED SPEED TRANSIENTS FIGURES 14 to 18

Values given based on full scale motor.

Run	Speed in rpm Initial	Final	Firing Angle Initial	Final	R_m in ohms.	i_3 amps.	R_a ohms.	T
J-1	902	320	96	135	111	2.0	52.0	6.7
J-2	460	742	127	109	111	2.0	6.2 10.4	1.12 1.81
K-1	205	430	137	121	26.9	2.8	7.3	1.10
K-2	728	465	97	120	26.9	2.8	12.4	1.62
L-1	490	210	106	132	9.6	2.8	18.2	1.20
L-2	365	590	118	97	9.6	2.8	3.1	0.45
N-1	408	825	104	62	5.2	2.8	0.57	0.10
N-2	830	388	60	108	5.2	2.8	6.7	0.56
P-1	715	885	70	52	4.0	3.9	0.57	0.96
P-3	880	680	52	74	4.0	3.9	2.8 0.48	0.31 0.096
Q-1	535	750	85	65	3.2	5.3	0.48	0.092
Q-2	875	778	51	63	3.2	5.3	0.48	0.092

Values for speeds, firing angles, R_m and i_3 taken from reference 4.

TABLE III

OPERATING CONDITIONS AND CIRCUIT PARAMETERS FOR
OBSERVED AND PREDICTED SPEED TRANSIENT FIGURES 14 to 18

Values given based on Full scale motor.

Run	Speed in rpm Initial	Final	Firing angle Initial	Final	L_m in cmm.	I_c amps.	R_m ohms.	T
J-1	902	320	96	135	111	2.0	52.0	6.7
J-2	460	742	127	109	111	2.0	6.2 10.4	1.12 1.51
E-1	205	430	137	121	26.9	2.8	7.3	1.10
K-2	728	465	97	120	26.9	2.6	12.4	1.62
L-1	490	210	106	132	9.6	2.8	18.2	1.20
L-2	365	590	118	97	9.6	2.8	3.1	0.45
M-1	408	625	104	82	5.2	2.8	0.37	0.10
M-2	830	388	60	108	5.2	2.8	6.7	0.56
P-1	715	885	70	52	4.0	3.9	0.57	0.96
P-3	880	680	52	74	4.0	3.9	2.8 0.48	0.31 0.096
Q-1	535	750	85	55	3.2	3.3	0.48	0.092
Q-2	875	778	51	63	3.2	3.3	0.48	0.092

Values for speeds, firing angles, L_m and I_c
based from reference 4.

ANALYTICAL DETERMINATION OF SPEED-TORQUE CURVES

In order to predict the speed transients for the ignitron-motor system by the methods previously described, it is necessary to obtain the speed-torque or counter-emf versus armature current curves of the motor for various ignitron firing angles. These may be obtained experimentally from the actual motor supplied by the ignitron rectifier from readings of direct current and voltage at the motor terminals corrected for the voltage drop through the armature resistance, or they may be obtained directly from an analogue circuit as described on pages 10 and 17.

An alternative method is available, however, for obtaining these curves directly from the machine constants of the d-c motor and the ignitron rectifier characteristics. For power applications in which a multi-phase rectifier is used, there will be two distinct regions to the performance curves, one for discontinuous conduction and the other for continuous conduction.

The phenomenon of discontinuous conduction where no current flows during portions of each cycle has been discussed in detail by Vedder and Puchlowski[1)] in connection with single-phase full-wave rectifiers. The continuous conduction condition where one of the rectifier tubes fires at the instant the tube in the preceding phase cuts off, and where the instantaneous current to the motor does not go to zero during any portion of the cycle has not been considered in such detail.

GRAPHICAL DETERMINATION OF MEAN-TORQUE CURVES

In order to predict the speed transients for the ignitron-motor system by the methods previously described, it is necessary to obtain the speed-torque or counter-emf versus armature current curves of the motor for various ignitron firing angles. These may be obtained experimentally from the actual motor supplied by the ignitron rectifier from readings of direct current and voltage at the motor terminals corrected for the voltage drop through the armature resistance, or they may be obtained directly from an analogue circuit as described on pages 10 and 17.

An alternative method is available, however, for obtaining these curves directly from the machine constants of the d-c motor and the ignitron rectifier characteristics. For power applications in which a multi-phase rectifier is used, there will be two distinct regions on the performance curves, one for discontinuous conduction and the other for continuous conduction.

The phenomenon of discontinuous conduction where no current flows during portions of each cycle has been discussed in detail by Yadder and Puncovec[1] in connection with single-phase full-wave rectifiers. The maximum conduction condition where one of the rectifier tubes fires at the instant the tube in the preceding phase cuts off, and where the instantaneous current to the motor does not go to zero during any portion of the cycle has not been considered in such detail.

Continuous Conduction.

For continuous conduction in the steady state and an arbitrary firing angle, the voltage applied to the motor terminals has the form shown in Figure 19. This may be compared with the oscillograms of Figure 4.

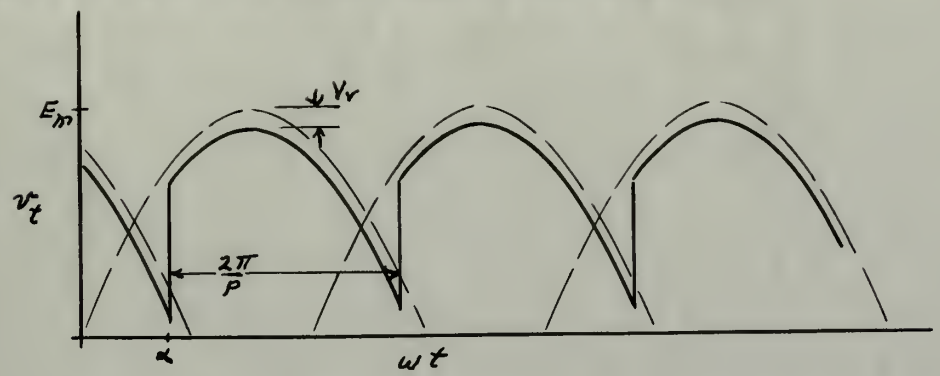

Figure 19. Motor Terminal Voltage for Continuous Conduction.

For a rectifier of p symmetrical phases, each tube is conducting over an interval of $\frac{2\pi}{p}$ and hence the applied voltage over one interval is given by

$$v_t = E_m \sin\omega t - V_r$$

$$\text{for} \quad \alpha < \omega t < \alpha + \frac{2\pi}{p}$$

where E_m = peak value of applied voltage to rectifier.

ω = 2π x line frequency.

V_r = rectifier tube voltage drop.

Since the phases are symmetrical, the applied voltage over each interval is the same and the average value of v_t over one interval is the direct voltage component applied to the motor. This may be found from

Continuous Conduction.

For continuous conduction in the steady state and an arbitrary firing angle, the voltage applied to the motor terminals has the form shown in Figure 19. This may be compared with the oscillograms of Figure 4.

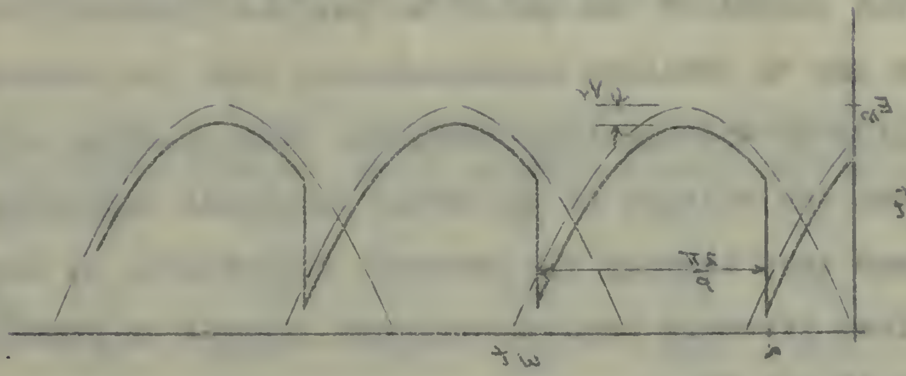

Figure 19. Motor Terminal Voltage for Continuous Conduction.

For a rectifier of p symmetrical phases, each tube is conducting over an interval of $\frac{2\pi}{p}$ and hence the applied voltage over one interval is given by

$$v_t = E_m \sin \omega t - V_r$$

$$\text{for} \quad \alpha < \omega t < \alpha + \frac{2\pi}{p}$$

Where E_m = peak value of applied voltage to rectifier.

ω = $2\pi \times$ line frequency.

V_r = rectifier tube voltage drop.

Since the phases are symmetrical, the applied voltage over each interval is the same and the average value of v_t over one interval is the direct voltage component applied to the motor. This may be found from

$$V_t = \frac{p}{2\pi}\int_{\alpha}^{\alpha+\frac{2\pi}{p}} (E_m \sin\omega t - V_r)\, d(\omega t)$$

$$= \frac{p}{2\pi} E_m\left[\cos\alpha - \cos\left(\alpha + \frac{2\pi}{p}\right)\right] - V_r$$

$$= \frac{p}{2\pi} E_m\left[\left(\cos\alpha - \cos\alpha\cos\frac{2\pi}{p} + \sin\alpha\sin\frac{2\pi}{p}\right)\right] - V_r$$

$$= p\frac{E_m}{2\pi}\left[\left(\cos\alpha\left(2\sin^2\frac{\pi}{p}\right) + \sin\alpha\left(2\sin\frac{\pi}{p}\cos\frac{\pi}{p}\right)\right)\right] - V_r$$

$$= p\frac{E_m \sin\pi/p}{\pi}(\sin\alpha + \pi/p) - V_r \qquad (27)$$

For continuous conduction, therefore, V_t with a given rectifier is a function only of the firing angle; and if the motor is assumed to have linear electrical characteristics, the counter-emf versus armature current relationship for each firing angle is given by the ordinary d-c motor equation.

$$E_b = V_t - I_a R_a - V_b \qquad (28)$$

where R_a = armature resistance of the motor

V_b = motor brush drop

The continuous conduction portion of the curves are thus a series of straight lines and can be plotted knowing only the effective armature resistance and the brush drop.

Discontinuous Conduction - Exact Method.

The shape of the curves where conduction is discontinuous may be determined accurately if required from the relationships derived by Vedder and Tuchlowski[1]; Harris[5] and Holler[4].

---

5. Harris, L. D., "Servomechanism Characteristics of D-C Motor Driven by Controlled Rectifiers", AIEE Technical Paper 51-297, July 1951.

$$V_c = \frac{p}{2\pi}\int_{\alpha}^{\alpha+\frac{2\pi}{p}} (I_m \sin\omega t \cdot \lambda_f) \, d(\omega t)$$

$$= \frac{p}{2\pi} I_m \lambda_f \left[\cos\alpha - \cos\left(\alpha + \frac{2\pi}{p}\right)\right] - \lambda_f^2$$

$$= \frac{p}{2\pi} I_m \left[(\cos\alpha - \cos\alpha\cos\tfrac{2\pi}{p} + \sin\alpha\sin\tfrac{2\pi}{p})\right] - \lambda_f^2$$

$$+ p\frac{I_m}{2}\left[\cos\alpha\left(\text{Zero}\tfrac{2\pi}{p}\right) + \sin\alpha\left|\text{zero}\tfrac{2\pi}{p}\right| \cos\tfrac{2\pi}{p}\right] - \lambda_f^2$$

$$= \frac{p I_m \sin\pi/p}{\pi}(\sin\alpha + \pi/\alpha) - \lambda_f^2 \qquad (27)$$

for continuous conduction, therefore, V_f =ifr + fixed resistor in a function both of the firing angle and if the motor is assumed to have linear electrical characteristics, the counter-emf versus armature current becomes particularly the easy firing angle is given by the ordinary d-c motor equation.

$$E_b = I_f - I_f R_a - V_f \qquad (28)$$

where E_b = armature resistance of the motor

E_f = motor drawn drop

The continuous conduction portion of the curves are thus a series of straight lines and can be closely counted only the effective armature resistance and the brush drop.

Discontinuous conducting - Open method.

The shape of the curves where conduction is discontinuous may be determined accurately by Method 1) ; Method 2) and Method 3).

---

3. Harris, F. D., "Quasi-Commutation Characteristics of D-C Motor Driven by Controlled Rectifier", AIEE Technical Paper 51-207, July 1951.

$$E_b = E_m \cos\theta_a \frac{(\sin(\alpha + \theta_a + r) - \varepsilon^{\frac{-r}{\tau_a}} \sin(\alpha + \theta_a)}{1 - \varepsilon^{-r/\tau_a}} - V_r - V_b \quad (29)$$

$$I_a = \frac{E_m}{R_a} \frac{2\pi}{p}\left[(\cos\alpha - \cos(\alpha + r) - \frac{E_b + V_r + V_b}{E_m} r)\right] \quad (30)$$

where $\theta_a = -\tan^{-1}\tau_a$

$$\tau_a = \frac{\omega L_a}{R_a}$$

r = angle during which conduction takes place

$$(r < \frac{2\pi}{p})$$

By taking values of α and r, E_b and I_a may be found to determine the desired points on the discontinuous portions of the performance curves. For the boundary condition between continuous and discontinuous conduction at a particular firing angle, $r = \frac{2\pi}{p}$, so that equation (30) reduces to the combination of equations (27) and (28), and equation (29) becomes

$$E_b = E_m \cos\theta_a \frac{(\sin(\alpha + \theta_a + \frac{2\pi}{p}) - \varepsilon^{-\frac{2\pi}{p\tau_a}} \sin(\alpha + \theta_a)}{1 - \varepsilon^{-\frac{2\pi}{p\tau_a}}} - V_r - V_b \quad (31)$$

Discontinuous Conduction - Approximate Method.

Using equations (29) and (30) involves considerable tedious calculation. However, it was found possible to approximate the discontinuous conduction performance curves for the system studied by assuming them to be simple parabolas of the form

$$I_a = k'(E_b \max - E_b)^2 \quad (32)$$

where $E_b \max = E_m - V_r - V_b$ (33)

for $\alpha \leq 90^\circ$

and $E_b \max = E_m \sin\alpha - V_r - V_b$ (34)

for $\alpha > 90^\circ$

$$e_b = E_m \cos\theta_a \frac{[\sin(\alpha + \theta_a + r) - \epsilon^{-\frac{r}{\vartheta_a}} \sin(\alpha + \theta_a)]}{1 - \epsilon^{-2\pi/p\vartheta_a}} - V_r - V_b \quad (29)$$

$$I_a = \frac{p E_m}{2\pi R_a}\left[\cos\alpha - \cos(\alpha + r) - \frac{e_b + V_r + V_b}{E_m} r\right] \quad (30)$$

where $\theta_a = -\tan^{-1}\vartheta_a$

$$\vartheta_a = \frac{\omega L_a}{R_a}$$

r = angle during which conduction takes place

$$\left(r < \frac{2\pi}{p}\right)$$

By taking values of α and r, e_b and I_a may be found to determine the desired points on the discontinuous portions of the performance curves. For the boundary condition between continuous and discontinuous conduction at a particular firing angle, $r = \frac{2\pi}{p}$, so that equation (30) reduces to the combination of equations (27) and (28), and equation (29) becomes

$$e_b = E_m \cos\theta_a \frac{\left(\sin(\alpha + \theta_a + \frac{2\pi}{p}) - \epsilon^{-\frac{2\pi}{p\vartheta_a}} \sin(\alpha + \theta_a)\right)}{1 - \epsilon^{-\frac{2\pi}{p\vartheta_a}}} - V_r - V_b \quad (31)$$

<u>Discontinuous Conduction - Approximate Method.</u>

Using equations (29) and (30) involves considerable tedious calculation. However, it was found possible to approximate the discontinuous conduction performance curves for the system studied by assuming them to be simple parabolas of the form

$$I_a = k'(e_b\,max - e_b)^2 \quad (32)$$

where $e_b\,max = E_m - V_r - V_b$ (33)

for $\alpha \leqq 90°$

and $e_b\,max = E_m \sin\alpha - V_r - V_b$ (34)

for $\alpha > 90°$

The constant k' is different for each firing angle and was determined by the fact that the discontinuous and continuous conduction curves for a given firing angle intersect at the point evaluated from equation (31).

The curves plotted on Figure 2 for firing angles up to 110° were obtained by this method and indicate very close agreement with the experimentally determined points shown. Since there can be no continuous conduction for firing angles of 120° or more with a three phase rectifier, the constant k' can not be evaluated under these conditions. Accordingly, the experimental points were used in drawing the curves for 130° and 150° on Figure 2. However, since k' appears to change slowly at large angles, these could have been obtained with some sacrifice in accuracy by assuming k' to have the same value as at 110°. This would probably be sufficiently accurate for most use, since this area of the curves is of little practical interest.

While it is obvious that this is a purely empirical method of obtaining the discontinuous conduction characteristics, it involves relatively simple calculations and is considered to be practicable for three-phase rectifiers used with motors having the same general characteristics as the unit used for this investigation. The end points for the curves are theoretically correct; but the actual shape of the intervening portion as given by equations (29) and (30) is a function primarily of the reactance to resistance ratio

of the motor armature circuit. The approximation presented here has been shown to be valid for one particular ratio and may not be entirely applicable to motors with different characteristics.

Effective Armature Resistance.

Determining the effective value of the armature resistance to be used in obtaining theoretical performance curves by any of the above methods is one of the major practical problems. As previously noted, the 60 cycle a-c resistance was used throughout this investigation; and although the justification for it is questionable, the theoretical and experimental results obtained show close agreement.

CONCLUSIONS

Analogue Circuit.

The analogue was originally proposed as a means of obtaining the steady state counter-emf versus armature current curves and for testing feedback arrangements to improve the transient speed response.

The results of the tests with the analogue circuit indicate that it represents the dynamic and steady-state behavior of the ignitron motor control system for all conditions except those involving operation in or near the boundary region between continuous and discontinuous conduction. However, since the operation of the circuit is actually unstable under these conditions, and since this region extends over a considerable portion of the characteristics, the usefulness of the analogue is limited.

It is not considered suitable for determining accurate steady-state characteristics, since the areas where the analogue does not give consistent results are the only ones of interest which cannot be easily obtained analytically.

Similarly, it is not considered practical for general use in feedback analysis because of its inherent instability over an appreciable portion of its operating range. However, it could be used for certain types of feedback investigations where stability is not involved.

CONCLUSIONS

Analogue Circuit.

The analogue was originally proposed as a means of obtaining the steady state counter-emf versus armature current curves and for testing feedback arrangements to improve the transient speed response.

The results of the tests with the analogue circuit indicate that it represents the dynamic and steady-state behavior of the ignitron motor control system for all conditions except those involving operation in or near the boundary region between continuous and discontinuous conduction. However, since the operation of the circuit is actually unstable under these conditions, and since this region extends over a considerable portion of the characteristics, the usefulness of the analogue is limited.

It is not considered suitable for determining accurate steady-state characteristics, since the areas where the analogue does not give consistent results are the only ones of interest which cannot be easily obtained analytically.

Similarly, it is not considered practical for general use in feedback analysis because of its inherent instability over an appreciable portion of the operating range. However, it could be used for certain types of feedback investigations where stability is not involved.

For the overall transient analysis problem, the method of predicting the response from a time constant derived from the steady-state characteristics of the system is considered easier and more practical for engineering investigations than either the use of an analogue circuit or the step by step analytical methods developed by Heller[4]. By using the approximate method for obtaining the steady-state characteristics for the system, this method reduces to a relatively simple analysis which nevertheless yields results of sufficient accuracy for nearly all purposes.

RECOMMENDATIONS

In spite of its limitations, the use of the analogue circuit is recommended for investigations leading toward the use of dynamic braking[3] to reduce the excessive slow-down times now required for an ignitron-fed motor.

If the analogue circuit is set up for this purpose, it is recommended that a high resistance be placed across the rectifier output with a view toward reducing the effects of the undesirable current cut-off transient encountered in this investigation.

For a determination of the servomechanisms characteristics of the ignitron control system, it is recommended that the work of Harris[5] be extended, using the concepts developed in this paper for the prediction of transient response, to include the condition encountered with three-phase rectifier where the speed-up and slow-down behavior are in general appreciably different.

In any theoretical or analogue circuit work with a rectifier-controlled d-c motor, the assumed value of the effective resistance of the armature of the motor to the average or direct component of the armature current has considerable influence on the results obtained. Since the d-c and a-c resistance of most motors differ so widely, it is recommended that a theoretical and experimental study be made to determine the effective value of armature resistance under these conditions and if necessary a practical means of obtaining it for a given machine.

CONCLUSIONS

In spite of its limitations, the use of the analogue circuit is recommended for investigations leading toward the use of dynamic braking[3] to reduce the excessive slow-down times now required for an ignitron-fed motor.

If the analogue circuit is set up for this purpose, it is recommended that a high resistance be placed across the rectifier output with a view toward reducing the effects of the undesirable overshoot out-of transient encountered in this investigation.

For a determination of the performance characteristics of the ignition control system, it is recommended that the work of Harris[5] be extended, using the concepts developed in this paper for the prediction of transient response, to include the condition encountered with three-phase rectifier where the speed-up and slow-down behavior are in general appreciably different.

In any theoretical or analogue circuit work with a rectifier-controlled d-c motor, the assumed value of the effective resistance of the armature of the motor to the average or mixed component of the armature current has considerable influence on the results obtained. Since the d-c and a-c resistances of most motors differ so widely, it is recommended that a theoretical and experimental study be made to determine the effective value of armature resistance under these conditions and if necessary a practical means of obtaining it for a given machine.

BIBLIOGRAPHY

1. Vedder, E. H. and Puchlowski, K. P., "Theory of Rectifier D-C Motor Drive", AIEE Trans., 62, 1943, pages 863-870.

2. Schmidt, A. and Smith, W. P., "Operation of Large D-C Motors from Controlled Rectifiers", AIEE Trans., 67, 1948, pages 679-683.

3. Chute, G. M., "Electronic Motor and Welder Controls", McGraw-Hill Book Co., 1951, pages 191-202, 226-277.

4. Heller, P. N., "Transient Speed and Armature Current Characteristics of an Ignitron-Fed D-C Motor", M.I.T. E.E. Dept. Thesis, 1951.

5. Harris, L. D., "Servomechanism Characteristics of D-C Motor Driven by Controlled Rectifiers", AIEE Technical Paper 51-297, July 1951.

BIBLIOGRAPHY

1. Vedder, J. D. and Van Sweden, C., "Theory of Rectifier D-C Motor Drive", AIEE Trans., 62, 1943, pages 863-870.

2. Schmidt, A. and Hyde, R. T., "Operation of Large D-C Motors from Controlled Rectifiers", AIEE Trans., 67, 1948, pages 679-683.

3. Chute, G. E., "Electronic Motor and Relay Control", McGraw-Hill Book Co., 1951, pages 193-203, 259-277.

4. Mellen, F. H., "Theoretical Speed and Armature Current Characteristics of an Ignitron-Fed D-C Motor", M.I.T. M.S. Dept. Thesis, 1951.

5. Nottia, L. D., "Servomechanism Characterization of D-C Motor Driven by Controlled Rectifier", AIEE Technical Paper 51-327, July 1951.

APPENDIX

APPENDIX

APPENDIX A

Nameplate data of motor and ignitron rectifier represented by the analogue circuit.

MOTOR

M.I.T. No. 250

Westinghouse

Type Sk, Frame 93	Style SC 1168256
15 horsepower	Serial 5SSC 1168256
56 amperes	230 volts D. C.
40°C Rise, continuous duty	850 rpm

GENERATOR

M.I.T. No. 251

Westinghouse

Type Sk, No. 90	Style 153133 B
18 horsepower	Serial no. 1556940
67 amperes	230 volts D. C.
780-1500 rpm	

RECTIFIER

M.I.T. No. 147

Westinghouse

Ignitron Rectifier

Input

18.75 kw 230 volt 60 cycle 3 phase

Output

230 volt 75 amperes D.C.

Serial 11P778

APPENDIX A

Nameplate data of motor and ignition rectifier transformer used by the auxiliary circuit.

MOTOR

B.I.T. No. 250

Westinghouse

Type SK, Frame 93 — Style 32 1168256

15 horsepower — Serial 3500 1168256

56 amperes — 230 volts D. C.

40°C Rise, continuous duty — 850 rpm

GENERATOR

B.I.T. No. 252

Westinghouse

Type SK, No. 90 — Style 1513J3 G

16 horsepower — Serial no. 1516942

67 amperes — 230 volts D. C.

780-1500 rpm

RECTIFIER

B.I.T. No. 147

Westinghouse

Ignitron Rectifier

Input

18.75 kw — 230 volt — 60 cycle — 3 phase

Output

230 volt — 75 amperes D.C.

Serial 771776

17139

Thesis B829 Bryant
Investigation of transients in an analogue circuit for an ignitron motor control system.